Organic & Biomolecular Chemistry

Accepted Manuscript

This article can be cited before page numbers have been issued, to do this please use: K. D. Paul, V. Luxami and I. Brar, *Org. Biomol. Chem.*, 2019, DOI: 10.1039/C8OB02973C.

ROYAL SOCIETY OF CHEMISTRY

rsc.li/obc

View Article Online
DOI: 10.1039/C8OB02973C

Synthesis and *in vitro* evaluation of naphthalimide-benzimidazole conjugates as potential antitumor agents

Iqubal Singh, Vijay luxami and Kamaldeep Paul*

School of Chemistry and Biochemistry, Thapar University, Patiala- 147 004, India

E-mail: kpaul@thapar.edu

Abstract

A series of novel naphthalimide-benzimidazole has been designed and synthesized for first time and studied for its effect on antiproliferative activity. Some of these compounds possessed good antitumor activity towards the tested cancer cell lines. Noticeably, (diethylamino)ethyl **15** and (dimethylamino)ethyl **23** derivatives displayed superior antiproliferative activity towards human cancer cell lines with MG_MID GI_{50} values of 1.43 and 1.83 μM, respectively. Preliminarily investigation reveals that compounds **15** and **23** might bind with ct−DNA through intercalation mode which is responsible for potent bioactivity. Moreover, transportation behaviour indicates that these molecules could efficiently bind and carried by bovine albumin, and the hydrogen bonding and hydrophobic interactions play important roles in interaction with serum albumin.

INTRODUCTION

DNA-damaging agent constitutes a cornerstone of cancer therapy and contributes to the subsistence of cancer patients in binding with drugs having different modes of interaction. However, the severe toxicity and drug resistance in clinic is the Achilles' heel of DNA-damaging agents.[1,2] Thus, by targeting DNA-associated processes, enhanced selectivity for cancer cells could be acquired. Naphthalimides are highly versatile functionalized moiety, and continuously receiving attention to bind with DNA,[3] thus establishing pronounced therapeutic importance in pharmaceutical and medicinal chemistry.[4,5] Some of the naphthalimides such as mitonafide, amonafide, and aristolochic acid showed effective antitumor activity towards the growth of various murine and human cancer cell lines. These naphthalimides exerted their anticancer function by interacting with DNA and inhibiting directly the function of replication and transcription, and/or topoisomerase (TOPO-II) to stabilize the supramolecular TOPO-II and DNA complex.[6] On account of limited efficacy and central neurotoxicity in solid tumors, the clinical developments of these compounds were regrettably terminated.[7,8] To increase the efficiency and toxicological

View Article Online
DOI: 10.1039/C8OB02973C

profile, significant efforts have been attempted for the development of more potent naphthalimides,[9-12] but most of these efforts were concentrated only on the binding affinity with DNA.[13] On the other hand, benzimidazole is an important structural motif for bioactivity and widely present in broad range of therapeutic drugs[14] having an electron-accepting group (C=N) and an electron-donating group (NH), that could rapidly interact with DNA and other useful biomacromolecules.[15] A large number of derivatives based on this moiety has been designed and evaluated for antitumor activity. Amongst these compounds, nocodazole, a 2-thienyl carbonyl benzimidazole, carbendazim, a benzimidazole carbamate and Veliparib, a pyrrolidine-2-yl benzimidazole are used in the clinic while mebendazole is currently undergoing clinical trials.[16] The biological potential of benzimidazoles against cancer cells has been reported with different mechanism of action. The success of these drugs and many other clinical trial derivatives[17] has provoked wide range of studies to construct more benzimidazole based bioactive molecules in the field of cancer. In view of these investigations, we have introduced benzimidazole fragment into C-4 position of naphthalimide ring to develop novel naphthalimide−benzimidazole conjugates. It is well known that functional groups present at the naphthalimide moiety especially at N-position are significantly affected the bioactivities of naphthalimide,[18] which might be beneficial for DNA and other targeting biomolecules. Aliphatic and aromatic amines *viz.*, (diethylamino)ethyl, (dimethylamino)ethyl, allylamine etc. are important structural appendages in improving and regulating the biological activities[19] and commonly present in number of clinical antitumor agents.[20] Rationally, in the present study, these moieties have been introduced at *N*-position of naphthalimide skeleton to investigate their effect on activity profile (**Figure 1**). The antitumor screenings with 60 human cancer cell lines were executed to naphthalimide-benzimidazoles **11-26.** Additionally, to study the effect of naphthalimide, the mode of action for anticancer activity was also evaluated through interaction with ct-DNA using different spectroscopic techniques. Cell cycle arrest was also checked to investigate the effect of benzimidazole using flow cytometer. The transportation behaviour of bovine serum albumin (BSA) to most active derivatives has also been done using UV-visible and fluorescence spectroscopy.

View Article Online
DOI: 10.1039/C8OB02973C

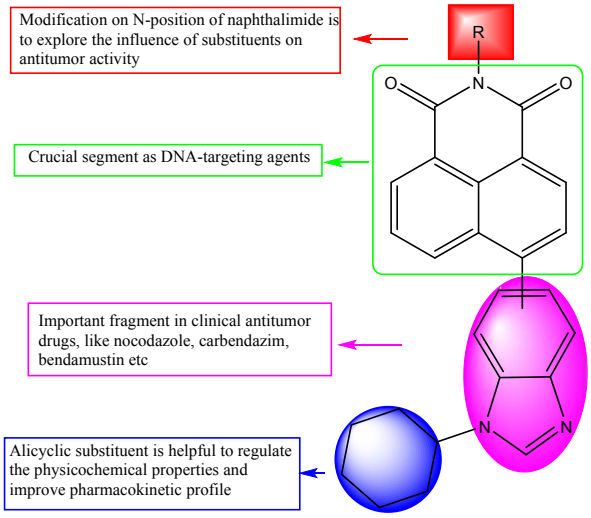

Figure-1 Design of novel naphthalimide-benzimidazoles

RESULTS AND DISCUSSION

Chemistry: Naphthalimide-benzimidazoles **11-26** have been synthesized via multistep reactions starting with commercial available 1,4- and 1,3-dibromobenzene according to **Scheme 1**. Nitration of 1,4- and 1,3-dibromobenzene **1a-b** with nitric acid and sulphuric acid in the ratio of 4:1, yielded 1,4-dibromo-2-nitro-benzene **2a** and 2,4-dibromo-1-nitro-benzene **2b** in 90% and 95% yields, both of which were subjected to regioselective nucleophilic substitution with cyclohexylamine to afford **3a-b**. Boronation of **3a-b** with bis(pinacolato)diboran in the presence of $Pd(PPh_3)_2Cl_2$ and KOAc, generated **4a-b**. Suzuki-Miyaura cross coupling of **4a-b** was carried out with 6-bromo-1*H*,3*H*-benzo[*de*]isochromene-1,3-dione **5** (obtained from bromination of acenaphthene followed by oxidation with potassium dichromate in glacial acetic acid) to obtain **6a-b**. Compound **6a-b** was further reduced with sodium dithionate in the presence of ammonia to afford mixture of **7a-b** and **8a-b** which were subsequently cyclized with triethylorthoformate in acetic acid at room temperature to afford the requisite **9a-b** and **10a-b**, respectively. The yields of both the intermediates were depended upon the amount of ammonia used in reduction. On refluxing of **9a-b** with alkyl and aryl amines in ethanol, compounds **11-26** were achieved in the yields of 71-86% **(Table 1)**. These novel synthesized compounds were well characterized by NMR and mass spectrometry (**Figures S1-S71**).

View Article Online
DOI: 10.1039/C8OB02973C

Scheme 1. Synthesis of 6-(1-cyclohexyl-1*H*-benzo[*d*]imidazol-5/6-yl)-2-substituted-1*H*-benzo[*de*]isoquinoline-1,3(2*H*)-dione

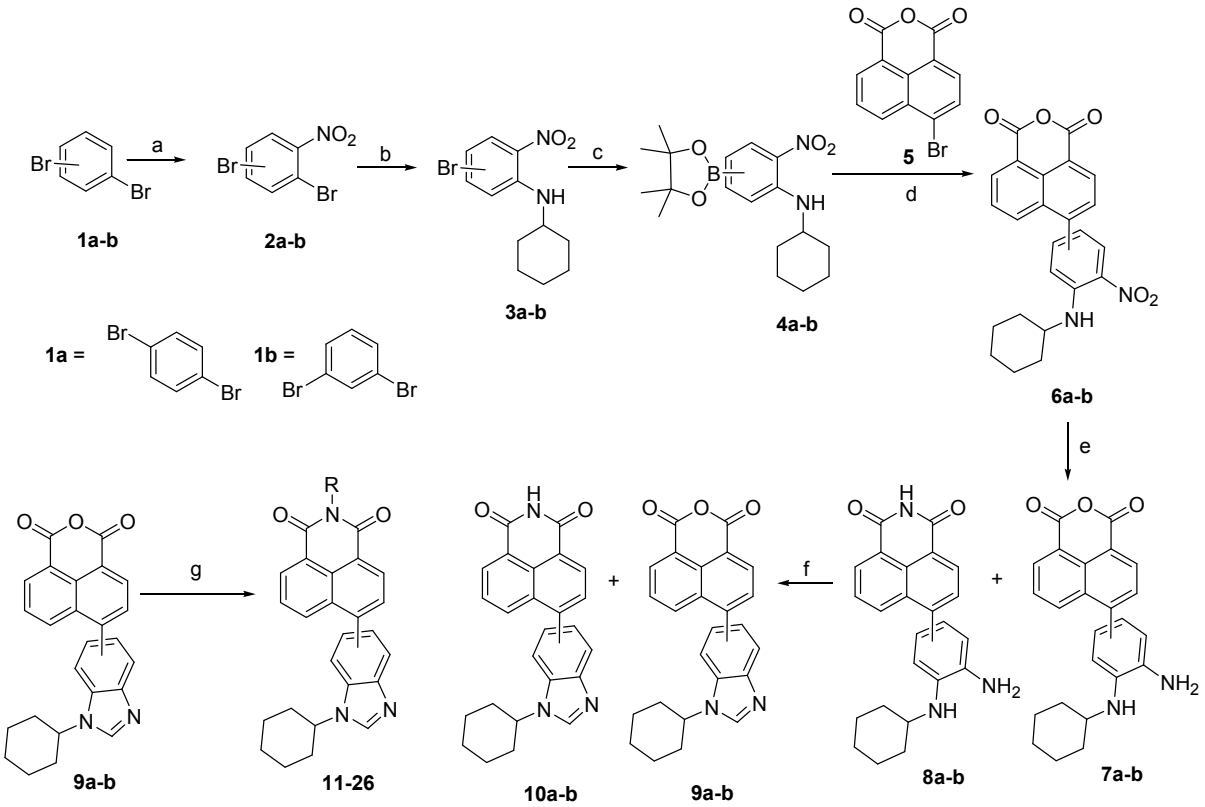

Reagents and conditions: (a) HNO_3, H_2SO_4, DCM, 0 °C, 30 min., 90-95%; (b) Cyclohexyl amine, K_2CO_3, DMF, 100 °C, 18 h, 70-75%; (c) Bis(pinacolato)diboron, $Pd(PPh_3)_2Cl_2$, KOAc, dioxane, reflux, 10 h, 78-82%; (d) $Pd(PPh_3)_4$, K_2CO_3, CH_3CN : water (9:1), N_2, reflux, 10-12 h, 70-73%; (e) $Na_2S_2O_4$, aq. NH_3, THF : water, 1 h, rt; (f) Triethylorthoformate, AcOH, 30 min., rt; (g) RNH_2, ethanol, reflux, 12-15 h, 71-86%.

Table 1. Photophysical properties of naphthalimide-benzimidazole conjugates

Compound	Starting Material	R	% yield	M.Pt. (°C)	Molecular Formulae
10a	**8a**	H	20	208-211	$C_{25}H_{21}N_3O_2$
10b	**8b**	H	25	213-216	$C_{25}H_{21}N_3O_2$
11	**9a**		76	261-263	$C_{28}H_{25}N_3O_2$
12	**9a**	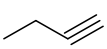	82	258-261	$C_{28}H_{23}N_3O_2$
13	**9a**	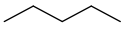	86	254-257	$C_{29}H_{29}N_3O_2$
14	**9a**	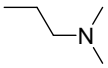	80	260-263	$C_{29}H_{30}N_4O_2$

View Article Online
DOI: 10.1039/C8OB02973C

15	**9a**	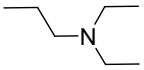	81	265-268	$C_{31}H_{34}N_4O_2$
16	**9a**	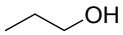	76	275-278	$C_{27}H_{25}N_3O_3$
17	**9a**	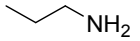	71	270-273	$C_{27}H_{26}N_4O_2$
18	**9a**	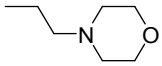	81	259-262	$C_{31}H_{32}N_4O_3$
19	**9a**	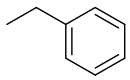	83	261-263	$C_{32}H_{27}N_3O_2$
20	**9a**	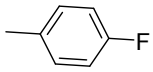	78	262-264	$C_{31}H_{24}FN_3O_2$
21	**9a**	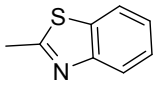	75	269-272	$C_{32}H_{24}N_4O_2S$
22	**9a**	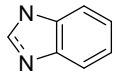	80	281-283	$C_{31}H_{24}N_4O$
23	**9b**	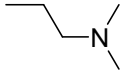	81	260-263	$C_{29}H_{30}N_4O_2$
24	**9b**	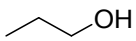	76	275-278	$C_{27}H_{25}N_3O_3$
25	**9b**	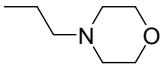	83	259-262	$C_{31}H_{32}N_4O_3$
26	**9b**	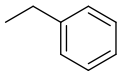	77	266-269	$C_{32}H_{27}N_3O_2$

Biological Activities. *Antiproliferative activity.* We are now interested to find out the effect of alkyl/aryl groups on naphthalimides towards the antiproliferative activity. National Cancer Institute (NCI)[21] has selected eighteen naphthalimide-benzimidazoles (**9a-b**, **10b, 11-23, 25** and **26**) for one-dose screening in the panel of 60 human cancer cell lines (**Tables S1-S2**). The results indicated that many of these naphthalimides exhibited equal or better antiproliferative activity than amonafide or mitonafide (drugs used in clinical trials). A comparison of the antiproliferative activities of two isomers of benzimidazole with naphthalimide revealed that derivatives substituted with aromatic rings were definitely less active than the aliphatic groups. In fact, amongst these eighteen naphthalimide-benzimidazoles, five showed antitumor effects in a broad range of cell lines at 10^{-5} M level and two of them showed antiproliferative activity with cytostatic and cytotoxic effects against all the 58 tested cell lines (**Table S3**). Compounds **15** and **23** fulfilled the selection

View Article Online
DOI: 10.1039/C8OB02973C

criteria set by NCI for antiproliferative activity in this assay and thus, selected for further evaluation at the full panel of cancer cell lines at five dose concentrations (10^{-4} – 10^{-8} M).

Three parameters for each cell line *viz.* GI_{50}, TGI and LC_{50} have been reported for derivatives **15** and **23** towards antitumor activity and average of mean graph midpoint (MG_MID) was determined for these parameters (**Figure S72-S73**). *In vitro* evaluation of these compounds indicated that derivatives **15** and **23** exhibited antitumor activity towards most of the human cell lines, showing MG_MID GI_{50} values of 1.43 and 1.83 μM, respectively **(Table 2)**. Both the derivatives showed particular efficacy against colon and leukemia subpanels having GI_{50} values in the range of 0.42-1.03 μM. The most sensitive leukemia and colon cell lines are MOLT-4 (GI_{50} = 0.44-0.47 μM) and HCT-116 (GI_{50} = 0.40-0.42 μM) for derivative **15** and SR (GI_{50} = 0.41-0.49 μM) and HT-29 (GI_{50} = 0.54-0.93 μM) in case of compound **23**, respectively. Moreover, derivative **15** exhibited good selectivity towards HOP-92 (GI_{50} = 0.37 μM) of non-small cell lung cancer, UO-31 (GI_{50} = 0.58 μM) of renal cancer and BT-549 (GI_{50} = 0.92 μM) of breast cancer while compound **23** showed selectivity towards LOX IMVI (GI_{50} = 0.82 μM) of melanoma cancer and ACHN (GI_{50} = 0.53 μM) of renal cancer. Thus, in the series of 5-benzimidazole series, (diethylamino)ethyl (**15**) indicated the better antitumor activity while in 6-benzimidazole series, (dimethylamino)ethyl (**23**) exhibited good activity. Overall, the naphthalimide substituted with 5-benzimidazole (**15**) led to more potency than the 6-benzimidazole analogue (**23**). These results were also compared with clinical trial drug, amonafide (NSC: 308847), a naphthalimide derivative and marketed drug nocadozaole (NSC: 238159), a benzimidazole analogue. It has been observed that compounds **15** and **23** are more active than amonafide but less potent than nocadozaole towards cancer cell lines.

Table 2: GI_{50} (μM), TGI (μM) and LC_{50} (μM) of derivatives **15** and **23** *in vitro* tumor cell lines

Comp.	Activity (μM)	I	II	III	IV	V	VI	VII	VIII	IX	MG_ MID[a]
15	**GI_{50}**	1.09	1.50	1.18	1.36	1.67	1.61	1.32	1.61	1.56	1.43
	TGI	4.94	3.39	3.07	2.89	3.15	4.14	3.39	3.93	3.97	3.65
	LC_{50}	[b]	10.8	6.74	5.72	5.85	13.8	11.2	53.2	5.84	14.1
23	**GI_{50}**	1.21	1.63	1.29	2.02	1.98	1.92	1.39	2.38	2.68	1.83
	TGI	7.87	6.19	8.89	11.6	5.47	12.1	7.05	9.62	14.2	9.24
	LC_{50}	[b]	44.6	58.5	55.3	35.6	67.2	29.5	53.1	66.4	51.3

View Article Online
DOI: 10.1039/C8OB02973C

Amonafide	**GI_{50}**	2.09	3.35	2.93	4.15	3.43	4.24	2.76	2.57	3.96	3.32
Nocodazole	**GI_{50}**	0.18	0.39	0.09	0.25	0.22	0.34	0.86	0.28	0.23	0.60

Leukemia (I), non-small cell lung cancer (II), colon cancer (III), CNS cancer (IV), melanoma (V), ovarian cancer (VI), renal cancer (VII), prostate cancer (VIII), breast cancer (IX). [a](MG_MID): The average sensitivity of all cell lines towards the test agent (μM), [b]Compounds showed values > 100 μM. GI_{50} = concentration for 50% of maximal inhibition of cell proliferation, TGI = concentration of the compound resulting in total growth inhibition, LC_{50} = lethal concentration required to kill 50% of the population.

DNA interaction studies. The binding properties of DNA with compounds **15** and **23** as a model of naphthalimide-benzimidazole conjugates have been studied with calf thymus (ct)-DNA using UV-visible and fluorescence spectroscopy as well as circular dichroism experiment.

UV-visible spectroscopic studies. Absorption spectroscopy is an effective technique to investigate the interaction mode of DNA with small molecule. Thus, in order to provide evidence for the possibility of binding of naphthalimide-benzimidazoles to calf-thymus DNA, UV-visible titrations of a solution of **15** and **23** with DNA have been performed. The absorption spectra of compounds **15** and **23** were exhibited absorption band at 370 nm in phosphate buffer (*p*H 7.4) at room temperature. The changes observed in the absorption spectra of compounds **15** and **23** (20.0 μM) with incremental addition of ct-DNA (0-110 μM for **15**; 0-85 μM for **23**), showed hypochromism at 370 nm (29.92 % for **15** and 20% for **23**), indicating the interaction of derivatives with double-helical ct-DNA (**Figure 2**). The absorption intensity at 370 nm has been decreased due to the fact that purine and pyrimidine bases of DNA are exposed because of binding of planar naphthalimide moiety with DNA. To access the stability of an adduct formed between DNA and substrate, Benesi-Hildebrand equation (Equation-1)[22] has been used to calculate the intrinsic binding constant (K_b) for compounds **15** and **23** (**Figure S74**) and were found to be 3.62×10^5 M^{-1}, R = 0.9847 and 2.23×10^5 M^{-1}, R = 0.9963, respectively. The results indicated that compound **15** with (diethylamino)ethyl showed strong interaction with ct-DNA than compound **23**.

View Article Online
DOI: 10.1039/C8OB02973C

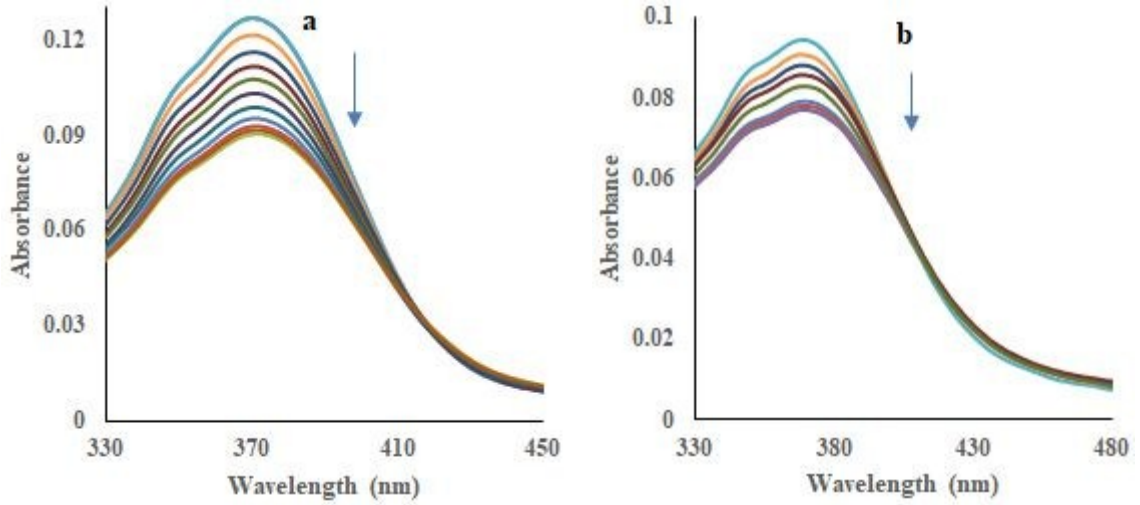

Figure 2. Absorption spectra of the compounds (a) **15** and (b) **23** (20.0 μM) in the presence of ct-DNA in phosphate buffer (*p*H 7.4) at 298 K

Thermal denaturation studies. Thermal behaviour of DNA in the presence of **15** and **23** might be given an insight into DNA conformation changes on rising the temperature, and thus offered information about the interaction strength of compounds with DNA. Generally, the intercalation of natural or synthetic organic intercalators results in considerable increase in melting temperature which is strongly correlated with the stability of double-helical ct-DNA.[23] The thermal denaturation experiment was carried out for DNA in the absence of compounds that revealed a T_m value of 75.6 ± 0.2 ˚C under our experimental conditions, whereas the melting temperature of DNA in the presence of compounds **15** and **23** were successively increased to 89.8 ± 0.2 ˚C and 81.5 ± 0.3 ˚C, respectively (**Figure S75**). The observed changes in UV-visible and T_m were consistent with the antitumor activity, with potency improving from compound **23** to **15**.

Fluorescence studies. Fluorescence emission of compounds **15** and **23** (5.0 μM) in aqueous solution showed a band at around 530 nm, at the excitation of 370 nm. Quenching of fluorescent intensity of compounds **15** (56.16 % at 298 K, 54.38 % at 308 K and 39.11 % at 318 K) and **23** (55.10 % at 298 K, 36.30 % at 308 K and 29.37 % at 318 K) at three different temperatures has been observed while maximum emission wavelength was slightly blue shifted to 20 nm with increase in the concentration of ct-DNA (**Figures 3** and **S76-S77)**. Quantitative estimation of quenching with DNA in terms of fluorescence quenching data was done by Stern-Volmer equation (Equation 2)[24] where K_{sv} and K_q have been calculated at different temperatures (**Table 3** and **Figures S78**). It has been observed that K_{sv} and K_q were decreased on increasing the temperature, indicated that the mechanism of quenching might be a static process. Moreover, the K_q is much

View Article Online
DOI: 10.1039/C8OB02973C

larger than diffusion controlled (1.0×10^{10} M^{-1} s^{-1})[25], also suggested that interaction involved the stating quenching. To calculate the binding constant (K_b) and the average number of binding sites per DNA molecule (n) of compound-DNA interaction, fluorescence titrations were performed at different temperatures using modified Stern-Volmer equation (Equation 3)[26] (**Figure S79**). The values of K_b were observed to decrease with increasing temperature for compounds **15** and **23,** indicating a reduction in the stability of the DNA-compound adduct at higher temperatures. The values of n have been obtained for both the compounds from the slope which were found to be close to one.

The non-covalent interactions between small molecule and ct-DNA are hydrogen bonding, electrostatic forces, hydrophobic interactions and van der Waals forces.[27] To determine these binding forces, thermodynamic parameters such as entropy change (ΔS), enthalpy change (ΔH) and free energy change (ΔG) have been calculated using van't Hoff equation (equations 4 and 5) (**Table 4, Figure S80**). The observed negative values of ΔG for compounds revealed that the binding process is spontaneous and favourable. The type of interaction between compound and DNA has been identified by evaluating the values of ΔH and ΔS and in the present study found to be -38.59 Kcal M^{-1} and -102.75 cal M^{-1} K^{-1} for compound **15**, and -27.36 Kcal M^{-1} and -67.40 cal M^{-1} K^{-1} for compound **23**, respectively. The negative values of ΔH and ΔS for **15** and **23** indicated that the interaction with DNA is mainly enthalpy driven by which hydrogen bonding and van der Waals contacts contributed towards the stability of complexes.

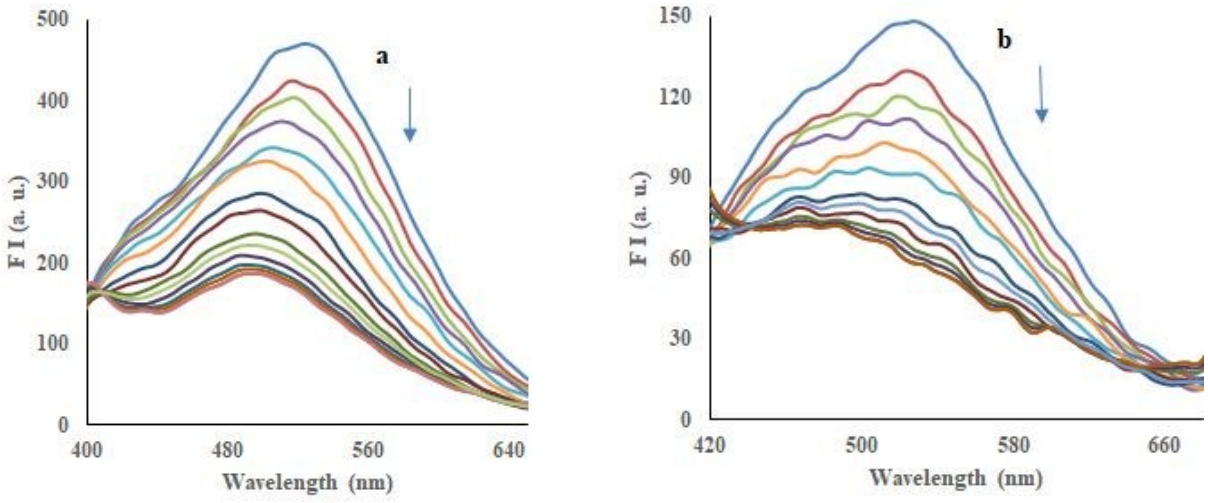

Figure 3. Emission spectra of compounds (a) **15** and (b) **23** in the presence of ct-DNA in phosphate buffer (*p*H 7.4) at 298 K

View Article Online
DOI: 10.1039/C8OB02973C

Table 3. Quenching and binding parameters for the interaction of compounds **15** and **23** with ct-DNA at three different temperatures

Compd	T (K)	K_{SV} ($\times10^4$) (M^{-1})	K_q ($\times10^{12}$) ($M^{-1}s^{-1}$)	R^2	K_b ($\times10^5$) (M^{-1})	n	R^2
15	298	4.72	4.72	0.9563	9.26	1.37	0.9856
	308	2.92	2.92	0.9597	0.49	1.06	0.9609
	318	1.72	1.72	0.9805	0.15	0.97	0.9686
23	298	5.98	5.98	0.9479	2.83	1.18	0.9352
	308	2.26	2.26	0.9497	0.29	1.03	0.9770
	318	1.88	1.88	0.9894	0.15	0.98	0.9931

Table 4. Thermodynamic parameters for the interaction of compounds **15** and **23** with ct-DNA at three different temperatures

Compd	T (K)	ΔH (Kcal M^{-1})	ΔS (cal M^{-1} K^{-1})	ΔG (Kcal M^{-1})	R^2
15	298	-38.59	-102.75	-7.9705	0.9502
	308			-6.943	
	318			-5.9155	
23	298	-27.36	-67.40	-7.2748	0.9178
	308			-6.6008	
	318			-5.9268	

Competitive displacement assay. To investigate the mode of binding of **15** and **23** to ct-DNA, a competitive binding experiment with ethidium bromide (EB) was performed. Ethidium bromide acts as one of the sensitive fluorescent probes having a planar structure that interacts with DNA by an intercalative mode.[28] Therefore, the relative affinity of compounds **15** and **23** to DNA was compared by examining their ability to displace EB from the DNA helix. Ethidium bromide shows an emission maximum at 600 nm on excitation at 520 nm. Fluorescence spectra of fixed concentration of EB-DNA complex (3 μM : 30 μM) in the presence of increasing concentration of compounds (**15**: 0-150 μM; **23**: 0-120 μM) in phosphate buffer (*p*H 7.4) were recorded (**Figure S81**). On subsequent addition of compounds, a decrease in fluorescence emission (**15**: 62.03% and **23**: 55.72%) at 600 nm of EB-DNA complex was observed indicated that these compounds were effectively competing with EB for the occupation at the same binding sites on DNA through intercalation.

View Article Online
DOI: 10.1039/C8OB02973C

Circular Dichroism (CD) studies. In order to get insight into the variations of properties induced by small molecule binding, CD spectroscopy is helpful in analysing the changes in DNA structure during DNA-drug interactions. The CD spectrum of DNA consists of a negative band at 247 nm because of helicity and a positive band at 277 nm due to base stacking, which are characteristics of DNA in the right handed B form.[29] As seen in **Figure 4** and **S82**, on the addition of compounds **15** and **23**, the intensities of positive and negative bands of DNA increased significantly; this observation is a strong indicator of classical intercalation. Moreover, these compounds did not yield positive induced CD (ICD) band at the region of (λ) 350 and 400 nm, instead of weak negative ICD band was observed, thus excluding binding into the minor groove of ct-DNA.[30-32] This data shows good agreement with increasing T_m and decreasing EB fluorescence intensity.

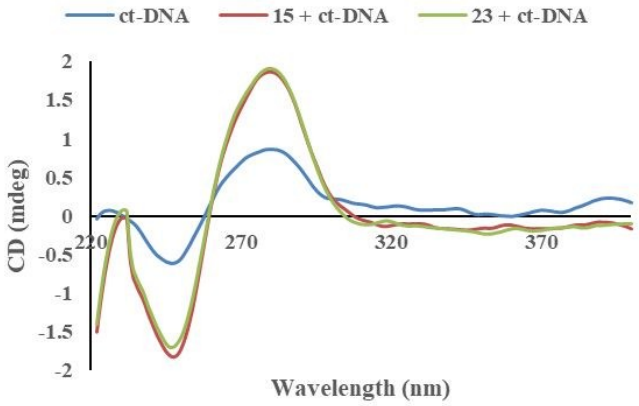

Figure 4. CD spectra of free ct-DNA (40 μM) (blue line), **15**-DNA complex (red line) and **23**-DNA complex (green line) at ratio $r_{[compound/ct\text{-}DNA]} = 0.025$ in Tris HCl buffer (pH 7.4)

Cell cycle analysis. Numerous anticancer compounds exhibit their effect by blockade of cell cycle process at a particular phase.[33] We hypothesized that naphthalimide-benzimidazole conjugates have the mechanism of action that they also arrest the process of mitosis. To test this hypothesis, we performed the cell cycle distribution using flow cytometer on the compounds **15** and **23** on MDA-MB-468 breast cancer cells. In our study, MDA-MB-468 cells were treated with compounds **15** and **23** at 1 μM concentration for 24 h along with control (without compound). The results indicated that compound **15** had no significant effect at cell cycle whereas compound **23** arrested the cell cycle at G_2/M phase (**Figure 5**, **Table 5**).

View Article Online
DOI: 10.1039/C8OB02973C

In the vehicle treated group, about 13.47% of MDA-MB-468 cells were distributed in G2/M phase. Only compound **23** increased the proportion of cells in G2/M phase. About 25.23% of cells were found in G2/M phase when treated with 1 μM of compound 23 for 24 h.

Table 5. Cell cycle distribution of MDA-MB-468 cell line treated with compounds **15** and **23**.

Compound	Sub G_1%	G_0/G_1%	S%	G_2/M%
Control	1.88	51.98	32.67	13.47
15	1.91	62.55	22.01	13.53
23	1.88	44.05	28.84	25.23

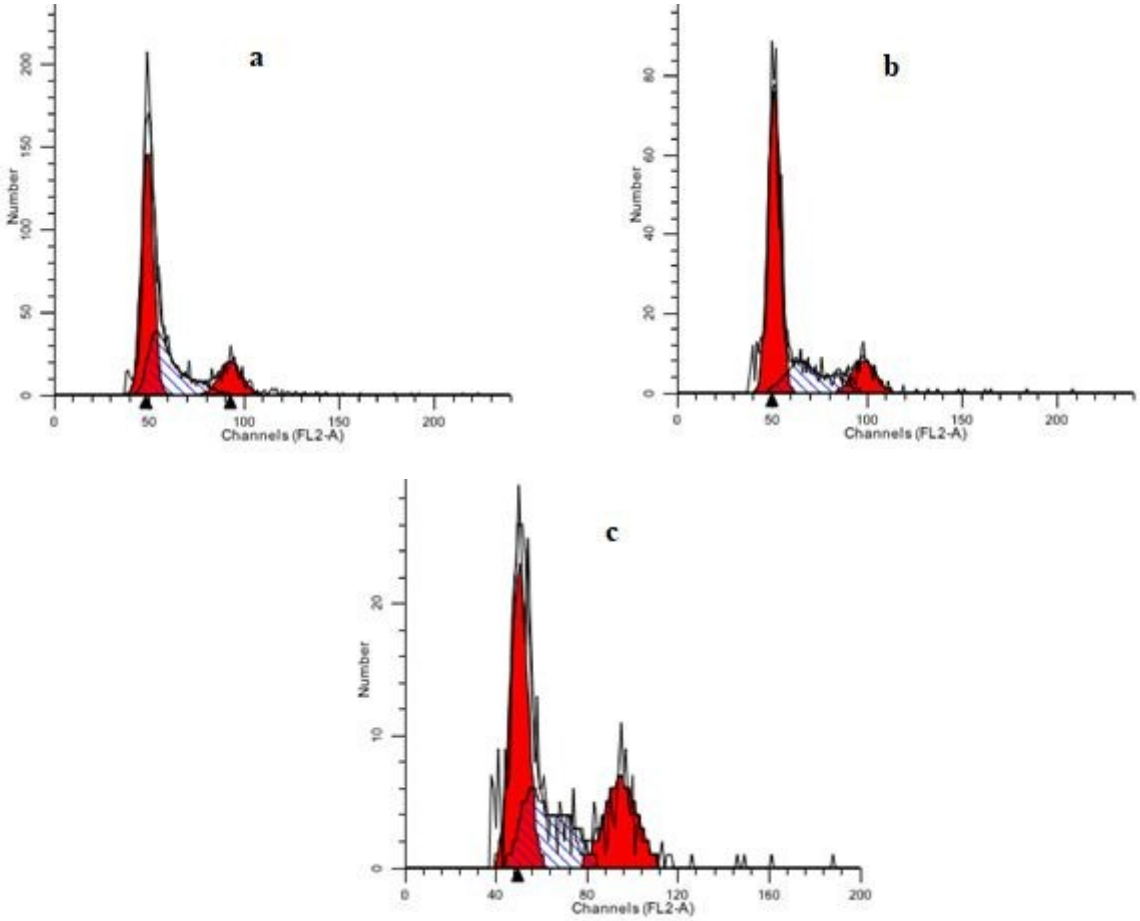

Figure 5. Flow cytometry analysis on cell cycle progression on MDA-MB-468 (breast cancer) cell line: (a) control, (b) compound **15** and (c) compound **23**.

BSA binding studies. Binding of a prospective drug to plasma protein is recognized as a crucial step in accessing its bioavailability,[34] and the reports on plasma protein binding are required in screening potential therapeutic agents.[35] Albumin binding, in particular, plays a decisive role

View Article Online
DOI: 10.1039/C8OB02973C

for *in vivo* bioavailability of any drug. Within this rationale, we examined the interaction of naphthalimide-benzimidazoles with bovine serum albumin (BSA), structural homology with human serum albumin (HSA), using absorption and emission titration experiments.

UV-visible spectroscopic studies. Absorption spectroscopy is used to explore the possibility of ground state interaction between drug and protein. Therefore, the interactions of derivatives with protein have been inferred from the changes in absorption spectra of serum albumin on gradual addition of compounds. UV-visible spectrum of BSA showed an intense absorption band at about 279 nm in phosphate buffer at *p*H 7.4, mainly due to the presence of tyrosine (Tyr), tryptophan (Trp) and phenylalanine (Phe) residues. On subsequent addition of compounds **15** and **23** (0-15 μM) to BSA solution (7.0 μM), gradual increase in intensity of band at 279 nm along with enhancement of new band at 370 nm was observed (**Figure 6**). These variations originated from changes in the conformation and the polarity of the microenvironment around aromatic residues of BSA. Moreover, the absorption maxima of BSA remains unchanged, suggested that the interactions between compounds and BSA are non-covalent in nature and likely to occur through π-π stacking between aromatics of naphthalimide-benzimidazole and phenyl rings of Trp, Tyr and Phe residues located in the binding cavity of BSA. Binding constants (K_b) for the interaction of compounds with BSA have been calculated using Benesi-Hildebrand equation (Equation 1)[22] and were found to be 6.96×10^4 M^{-1} for **15** and 5.64×10^4 M^{-1} for **23 (Figure S83)**, signifying better binding affinity of compound **15** with serum albumin than **23**.

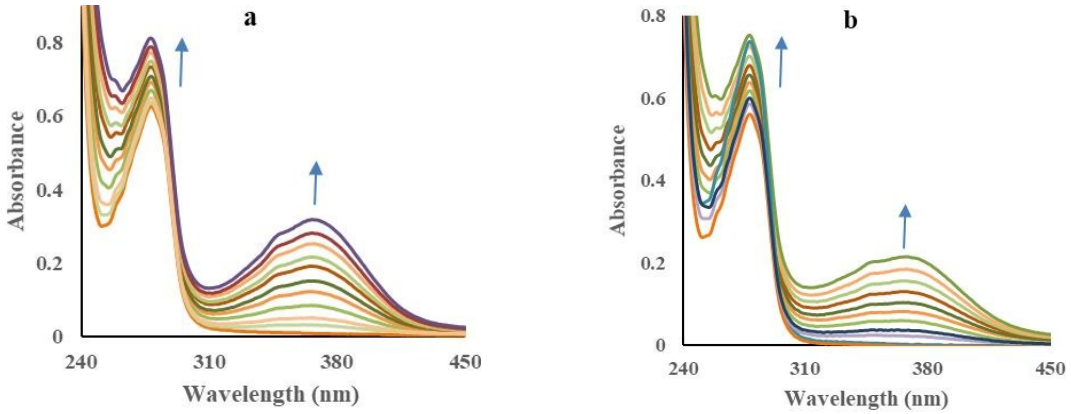

Figure 6. Absorption spectra of BSA in the presence of compounds (a) **15** and (b) **23** in phosphate buffer (*p*H 7.4) at 298 K.

Fluorescence studies. The observations obtained from absorption studies are not sufficient to determine the interaction of compounds in detail. Therefore, emission spectroscopy has been

View Article Online
DOI: 10.1039/C8OB02973C

preferred for reviewing binding mode of interactions. The emission of BSA is observed from two Trp residues; one of them is located on the surface and the other residue present in the hydrophobic pocket of protein molecule.[36] **Figure 7** depicts that on progressive addition of different concentration of compounds (0-45 μM) to BSA (7.0 μM), the emission spectrum of Trp residues of serum protein at around 350 nm was gradually quenched (82.49% for **15** and 79.11% for **23**) with the appearance and enhancement of new band at 485 nm. The λ_{max} of the emission of Trp residues in BSA was also blue shifted from 350 nm (in free BSA) to 330 nm. This suggests that the emitting Trp residue(s) in the complex of compound-BSA are in less polar or more hydrophobic environment as compared with free BSA.

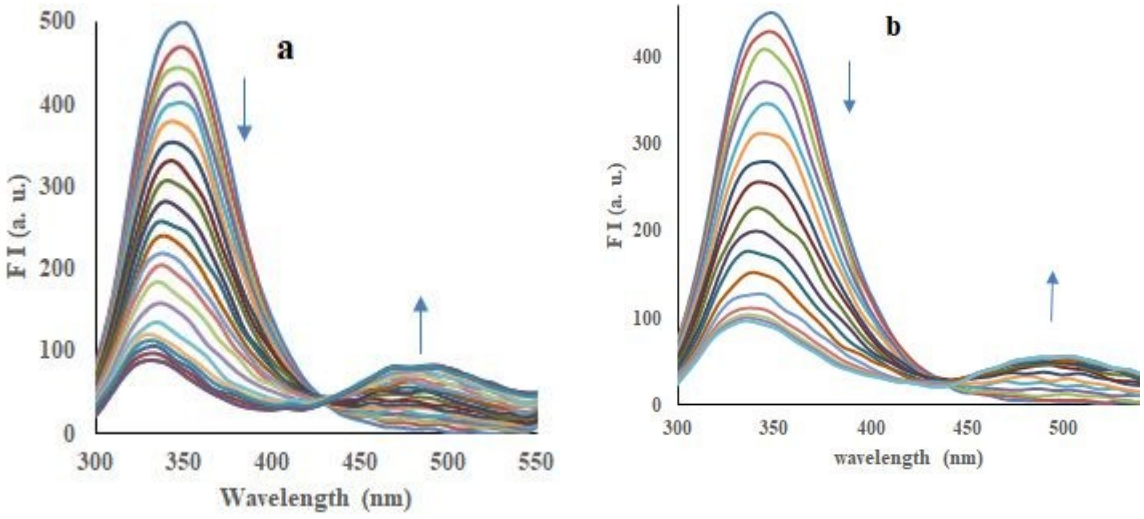

Figure 7. Emission spectra of BSA in the presence of compounds (a) **15** and (b) **23** in phosphate buffer (*p*H 7.4) at 298 K

The steady-state fluorescence quenching of Trp emission in serum albumin with addition of compound has been characterized by Stern-Volmer equation (equation 2)[24] that showed the relation between the quenching extent for each compound and the strength of their interactions with BSA. The values of Stern-Volmer constant (K_{SV}) and bimolecular quenching constant (K_q) were calculated from the slope of linear portion of regression curve using equation 2 (**Table 6** and **Figure S84a**). A linear Stern-Volmer plot was obtained with compounds **15** and **23,** suggesting that solely one type of quenching or binding process occur, either stating or dynamic quenching. The values obtained for bimolecular quenching constant (K_q) of compounds **15** (1.41×10^{13} $M^{-1}s^{-1}$) and **23** (1.52×10^{13} $M^{-1}s^{-1}$) were much greater than the diffusion control limited value of 1×10^{10} M^{-1} s^{-1}, which is the largest possible value reported in aqueous medium.[25] Thus, the binding of

View Article Online
DOI: 10.1039/C8OB02973C

compounds to BSA probably involves the stating quenching with formation of complex at ground state.

Modified Stern-Volmer equation (Equation 3)[26] has been used to determine the binding constant (K_b) and the average number of binding sites (n) for compound-BSA complexes (**Figure S84b**). These complexes exhibited excellent binding parameters, suggesting their binding to the albumins and their possible transfer as well as their release ability upon arrival at their target sites. As these values are significantly lower than 10^{15} M^{-1}, which is the value of the association constant of the protein albumin with diverse compounds; their interactions are considered significant among the known non-covalent ones.[37]

Table 6. Quenching and binding parameters for interaction of BSA with compounds **15** and **23**

Compd	K_{sv} ($\times10^5$)(M^{-1})	K_q ($\times10^{13}$) ($M^{-1}s^{-1}$)	R^2	K_b ($\times10^5$)(M^{-1})	n	R^2
15	1.41	1.41	0.9808	9.34	1.23	0.9971
23	1.52	1.52	0.9903	1.41	1.02	0.9956

CONCLUSION

A series of isomeric benzimidazole with substituted naphthalimides has been synthesized in moderate to good yields and studied their effects on antiproliferative activity. Both the isomeric groups of 18 compounds were assessed over 60 human tumor cell line panel at 10^{-5} M concentration, where most of the examined compounds showed superior activity. Compounds **15** and **23** were identified higher activity against leukemia and colon cancer subpanels at five dose concentration levels. The interaction between these compounds with DNA was studied by UV-visible, fluorescence and CD spectroscopy as well as DNA melting experiment. The results suggested that the fluorescence of compounds **15** and **23** has been quenched significantly by DNA and the probable mechanism was a stating quenching process. The association constant (K_b) value between compound and DNA was in the order of 10^5 mol^{-1}, which is better than other reported DNA intercalators. The thermodynamic parameters, ΔH^o and ΔS^o, were calculated in the range of -38.59 to -27.36 Kcal M^{-1} and -102.75 to -67.40 cal M^{-1} K^{-1}, respectively, indicated that the binding of compounds to DNA were driven mainly by hydrogen bonds and van der Waals interactions. Mechanism of action studies with cell cycle arrest confirmed that compound **23** maintained their ability to arrest cells in G2/M phase and induce cell apoptosis. Compounds **15** and **23** have also been effectively bound to BSA protein with good binding constant values of 9.34 x 10^5 M^{-1} and

View Article Online
DOI: 10.1039/C8OB02973C

1.41 x 10^5 M^{-1}, respectively, determined through emission spectroscopy. Thus, naphthalimide-benzimidazole molecules with a superior bioactivity profile and mode of interaction with DNA and BSA have been described, and objective is completely satisfied.

EXPERIMENTAL SECTION

Chemistry. *General Methods.* All commercially available compounds (Spectrochem, Aldrich, Merck etc.) were used without purification. Melting points were determined in an open capillary and were uncorrected. ^1H and ^{13}C NMR spectra have been performed on Jeol ECS 400 NMR spectrophotometer, which were operated at 400 MHz for ^1H nuclei and 100 MHz for ^{13}C nuclei, using $CDCl_3$ as solvent. Chemical shifts are reported in parts per million (ppm) with TMS as an internal reference. Water Micromass-Q-T of Micro has been used to determine the mass Spectra. CHN analysis was done using Thermo Scientific (Flash 2000) analyser. Reactions have been observed by TLC with plate coated with silica gel HF-254 and column chromatography was done with silica gel 60-120/100-200 mesh. UV-visible absorption and fluorescence emission spectra were measured with 1 cm quartz cell. Shimadzu-2400 PC spectrometer instrument was used to determine the UV-visible spectra. Emission spectra were recorded with Varian Cary Eclipse fluorescence spectrometer. Circular dichroism spectra were recorded with an Applied Photophysics CD spectrophotometer.

*Synthesis of dibromonitrobenzene (**2a-b**)*:[38] Dibromobenzene (**1a-b**) (5 g, 21.27 mmol) in dichloromethane (15 ml) and sulphuric acid (10 ml) was treated with cooled solution of nitric acid and sulphuric acid (4:1) at 0˚C for 30 min. The reaction mixture was allowed to warm at room temperature with stirring. On completion of reaction (monitored by TLC), quenched the reaction mixture with ice. The precipitate formed was collected and dried in an oven to afford desired product **(2a-b)** in 90-95% yields.

*Synthesis of 4/5-bromo-N-cyclohexyl-2-nitroaniline (**3a-b**)*: Dibromonitrobenzene (3 g, 10.71 mmol), cyclohexyl amine (1.27 g, 12.85 mmol) and K_2CO_3 (1.47 g, 10.71 mmol) were taken in DMF (20 ml) in 100 ml dried round bottom flask and stirred the reaction mixture at 100˚C for 18 h. On completion of reaction, 50 mL water was added and extracted with ethyl acetate. The extract was then dried over anhydrous sodium sulphate, filtered and concentrated to get the crude product. The residue was column purified on silica gel (Hexane/EtOAc = 20:1) to obtain the desired product.

View Article Online
DOI: 10.1039/C8OB02973C

*4-Bromo-N-cyclohexyl-2-nitroaniline (**3a**)*: Yellow solid; 75% yield; mp 93-96 ^{o}C; ^{1}H NMR ($CDCl_3$, 400 MHz): δ (ppm) 8.27 (d, J = 2.32 Hz, 1H, ArH), 8.12 (d, J = 7.36 Hz, 1H, NH), 7.44 (dd, ^{2}J = 9.16 Hz, ^{3}J = 2.28 Hz, 1H, ArH), 6.79 (d, J = 9.16 Hz, 1H, ArH), 3.52-3.43 (m, 1H, cyclohex-CH), 2.04-2.02 (m, 2H, cyclohex-CH_2), 1.82-1.78 (m, 2H, cyclohex-CH_2), 1.69-1.62 (m, 1H, cyclohex-CH_2), 1.47-1.25 (m, 5H, cyclohex-CH_2); ^{13}C NMR ($CDCl_3$, 100 MHz): δ (ppm) 143.5, 138.6, 131.6, 128.8, 115.8, 105.6 (ArC), 51.0 (CH), 32.4 (CH_2), 25.3 (CH_2), 24.3 (CH_2).

5-Bromo-N-cyclohexyl-2-nitroaniline (***3b***)**:** Yellow solid; 70% yield; mp 90-93 ^{o}C; ^{1}H NMR ($CDCl_3$, 400 MHz): δ (ppm) 8.13 (d, J = 6.88 Hz, 1H, NH), 8.00 (d, J = 9.16 Hz, 1H, ArH), 7.01 (d, J = 1.84 Hz, 1H, ArH), 6.69 (dd, ^{2}J = 9.16 Hz, ^{3}J = 2.28 Hz, 1H, ArH), 3.49-3.42 (m, 1H, cyclohex-CH), 2.05-2.02 (m, 2H, cyclohex-CH_2), 1.82-1.74 (m, 2H, cyclohex-CH_2), 1.68-1.64 (m, 1H, cyclohex-CH_2), 1.49-1.28 (m, 5H, cyclohex-CH_2); ^{13}C NMR ($CDCl_3$, 100 MHz): δ (ppm) 144.8, 131.4, 130.3, 128.1, 117.9, 116.4 (ArC), 50.9 (CH), 32.4 (CH_2), 25.3 (CH_2), 24.3 (CH_2).

Synthesis of N-cyclohexyl-2-nitro-4/5-(4,4,5,5-tetramethyl-1,3,2-dioxaborolan-2-yl)aniline (***4a-b***): 4/5-Bromo-*N*-cyclohexyl-2-nitroaniline (**3a-b**) (2.0 g, 6.68 mmol), bis(pinacolato)diboron (2.03 g, 8.01 mmol), KOAc (0.98 g, 10.01 mmol), palladium(II)bis(triphenylphosphine) dichloride (5.0 mol%) in 1,4-dioxane (30 mL) were charged in 100 ml oven-dried round bottom flask. The reaction mixture was refluxed for 10 h until the halide was completely consumed as determined by TLC. The mixture was then cooled to room temperature. Solvent of reaction was concentrated under reduced pressure and the crude was extracted with chloroform and water (3 × 50 mL). The extract was dried over anhydrous Na_2SO_4, filtered and concentrated. The crude material obtained was column purified on silica gel using ethyl acetate and hexane to obtain the desired reddish yellow product.

*N-Cyclohexyl-2-nitro-4-(4,4,5,5-tetramethyl-1,3,2-dioxaborolan-2-yl)aniline (**4a**)*: Reddish yellow solid; 82% yield; mp 125-127 ^{o}C; ^{1}H NMR ($CDCl_3$, 400 MHz): δ (ppm) 8.63 (d, J = 1.36 Hz, 1H, ArH), 8.29 (d, J = 6.88 Hz, 1H, NH), 7.75 (dd, ^{2}J = 8.68 Hz, ^{3}J = 0.92 Hz, 1H, ArH), 6.83 (d, J = 8.72 Hz, 1H, ArH), 3.58-3.51 (m, 1H, cyclohex-CH), 2.06-2.03 (m, 2H, cyclohex-CH_2), 1.82-1.76 (m, 2H, cyclohex-CH_2), 1.67-1.63 (m, 1H, cyclohex-CH_2), 1.48-1.23 (m, 17H, cyclohex-CH_2 & boronate-CH_3); ^{13}C NMR ($CDCl_3$, 100 MHz): δ (ppm) 146.1, 141.3, 134.5, 131.4, 113.2 (ArC), 83.7 (C), 50.8 (CH), 32.5 (CH_2), 25.4 (CH_2), 24.7 (CH_3), 24.4 (CH_2).

*N-Cyclohexyl-2-nitro-5-(4,4,5,5-tetramethyl-1,3,2-dioxaborolan-2-yl)aniline (**4b**):* Reddish yellow solid; 78% yield; mp 120-122 ^{o}C; ^{1}H NMR ($CDCl_3$, 400 MHz): δ (ppm) 8.13 (d, J = 8.68

View Article Online
DOI: 10.1039/C8OB02973C

Hz, 2H, NH & ArH), 7.28 (s, 1H, ArH), 6.96 (d, J = 8.72 Hz, 1H, ArH), 3.71-3.63 (m, 1H, cyclohex-CH), 2.07-2.02 (m, 2H, cyclohex-CH_2), 1.83-1.76 (m, 2H, cyclohex-CH_2), 1.67-1.63 (m, 1H, cyclohex-CH_2), 1.53-1.28 (m, 17H, cyclohex-CH_2 & boronate-CH_3); ^{13}C NMR ($CDCl_3$, 100 MHz): δ (ppm) 143.8, 135.5, 132.6, 125.7, 120.8, 119.9 (ArC), 84.3 (C), 50.3 (CH), 32.7 (CH_2), 25.5 (CH_2), 24.7 (CH_3), 24.3 (CH_2).

Synthesis of 6-(4/3-(cyclohexylamino)-3/4-nitrophenyl)-1H,3H-benzo[de]isochromene-1,3-Dione (***6a-b***): To a solution of 6-bromo-1*H*,3*H*-benzo[*de*]isochromene-1,3-dione (**5**) (2 g, 7.22 mmol) in a mixture of acetonitrile and water (9:1) in 100 ml round bottom flask, *N*-cyclohexyl-2-nitro-4/5-(4,4,5,5-tetramethyl-1,3,2-dioxaborolan-2-yl)aniline (**4a-b**) (2.51 g, 7.22 mmol) and K_2CO_3 (1.0 g, 7.22 mmol) were added under inert atmosphere. Then, $Pd(PPh_3)_4$ (5 mol%) was added with continued N_2 purging and refluxed the reaction mixture for 10-12 h. On completion of reaction (determined by TLC), solvents were evaporated under reduced pressure followed by water (50 ml) was added and then extracted with chloroform. Chloroform layer was dried over sodium sulphate. The crude product has further been purified by column chromatography with hexane and ethylacetate to get the yellowish solid product.

6-(4-(Cyclohexylamino)-3-nitrophenyl)-1H,3H-benzo[de]isochromene-1,3-dione (***6a***): Reddish yellow solid; 70% yield; mp 83-86 ^{o}C; ^{1}H NMR ($CDCl_3$, 400 MHz): δ (ppm) 8.67-8.63 (m, 2H, ArH), 8.42 (dd, ^{2}J = 8.72 Hz, ^{3}J = 0.92 Hz, 1H, ArH), 8.39 (d J = 2.28 Hz, 1H, ArH), 8.35 (d, J = 7.36 Hz, 1H, ArH), 7.82-7.78 (m, 1H, ArH), 7.76 (d, J = 7.76 Hz, 1H, ArH), 7.61 (dd, ^{2}J = 8.72 Hz, ^{3}J = 1.84 Hz, 1H, ArH), 7.11 (d, J = 9.16 Hz, 1H, NH), 3.68-3.59 (m, 1H, Cyclohex-CH), 2.16-2.12 (m, 2H, Cyclohex-CH_2), 1.89-1.82 (m, 2H, Cyclohex-CH_2), 1.73-1.69 (m, 1H, Cyclohex-CH_2), 1.53-1.43 (m, 4H, Cyclohex-CH_2), 1.41-1.33 (m, 1H, Cyclohex-CH_2); ^{13}C NMR ($CDCl_3$, 100 MHz): δ (ppm) 160.6, 160.4, 146.3, 144.6, 137.0, 133.5, 133.4, 133.1, 131.4, 131.0, 130.0, 128.2, 128.0, 127.4, 124.2, 118.9, 117.4, 114.9 (ArC), 51.3 (CH), 32.6 (CH_2), 25.4 (CH_2), 24.5 (CH_2).

6-(3-(Cyclohexylamino)-4-nitrophenyl)-1H,3H-benzo[de]isochromene-1,3-dione (***6b***): Reddish yellow solid; 73% yield; mp 81-84 ^{o}C; ^{1}H NMR ($CDCl_3$, 400 MHz): δ (ppm) 8.65 (t, J = 6.44 Hz, 2H, ArH), 8.35 (t, J = 7.32 Hz, 2H, ArH), 8.31 (d, J = 7.80 Hz, 1H, ArH), 7.83-7.78 (m, 2H, ArH), 6.99 (s, 1H, NH), 6.72 (dd, ^{2}J = 8.72 Hz, ^{3}J = 1.36 Hz, 1H, ArH), 3.60-3.52 (m, 1H, Cyclohex-CH), 2.10-2.06 (m, 2H, Cyclohex-CH_2), 1.82-1.77 (m, 2H, Cyclohex-CH_2), 1.68-1.62 (m, 1H, Cyclohex-CH_2), 1.50-1.32 (m, 5H, Cyclohex-CH_2); ^{13}C NMR ($CDCl_3$, 100 MHz): δ (ppm)

View Article Online
DOI: 10.1039/C8OB02973C

160.3, 160.1, 146.7, 145.7, 144.5, 133.5, 132.8, 131.3, 130.5, 129.8, 127.8, 127.7, 127.5, 118.8, 118.4, 116.1, 115.2 (ArC), 51.0 (CH), 32.6 (CH_2), 25.4 (CH_2), 24.3(CH_2).

*Synthesis of 6-(3/4-amino-4/3-(cyclohexylamino)phenyl)-1H,3H-benzo[de]isochromene-1,3-dione (**7a-b**) and 6-(3/4-amino-4/3-(cyclohexylamino)phenyl)-1H-benzo[de]isoquinoline-1,3(2H)-dione (**8a-b**):* A 100 ml round bottom flask was charged with 6-(4/3-(cyclohexylamino)-3/4-nitrophenyl)-1*H*,3*H*-benzo[*de*]isochromene-1,3-dione (**6a-b**) (2 g, 4.80 mmol) and sodium dithionite (4.18 g, 24.03 mmol) in THF:water (3:2). Ammonia solution (5 ml) has been added to the reaction mixture and stirred for 1 h at room temperature. Completion of reaction was monitored by TLC and the reaction mixture was extracted with ethyl acetate. Ethyl acetate layer was dried over Na_2SO_4, filtered and concentrated to get the crude product. Mixture of crude brown product (**7** and **8**) was directly used further without purification.

*Synthesis of 6-(1-cyclohexyl-1H-benzo[d]imidazol-5/6-yl)-1H,3H-benzo[de]isochromene-1,3-dione (**9a-b**) and 6-(1-cyclohexyl-1H-benzo[d]imidazol-5/6-yl)-1H-benzo[de]isoquinoline-1,3(2H)-dione (**10a-b**)*: Mixture of 6-(3/4-amino-4/3-(cyclohexylamino)phenyl)-1*H*,3*H*-benzo[*de*]isochromene-1,3-dione (**7a-b**) and 6-(3/4-amino-4/3-(cyclohexylamino)phenyl)-1*H*-benzo[*de*]isoquinoline-1,3(2*H*)-dione (**8a-b**) (1 mmol) was stirred with triethylorthoformate (1 mmol) in acetic acid (30 ml) for 30 min at room temperature. The reaction mixture was then poured into water and then treated with $NaHCO_3$ followed by extracted with chloroform. Sodium sulphate was used to dry the chloroform layer. Crude was purified by column chromatography using ethyl acetate and hexane as elutents to obtain light brown solid.

*6-(1-Cyclohexyl-1H-benzo[d]imidazol-5-yl)-1H,3H-benzo[de]isochromene-1,3-dione (**9a**)*: Light brown solid; 72% yield; mp 191-193 ^oC; ^1H NMR ($CDCl_3$, 400 MHz): δ (ppm) 8.65 (d, J = 7.32 Hz, 1H, ArH), 8.62 (d, J = 7.32 Hz, 1H, ArH), 8.46 (d, J = 8.68 Hz, 1H, ArH), 8.16 (s, 1H, ArH), 7.92 (s, 1H, ArH), 7.81 (d, J = 7.32 Hz, 1H, ArH), 7.74 (t, J = 8.44 Hz, 1H, ArH), 7.66 (d, J = 8.24 Hz, 1H, ArH), 7.45 (dd, ^2J = 8.28 Hz, ^3J = 1.40 Hz, 1H, ArH), 4.36-4.28 (m, 1H, cyclohex-CH), 2.33 (d, J = 11.00 Hz, 2H, cyclohex-CH_2), 2.08-2.03 (m, 2H, cyclohex-CH_2), 1.95-1.85 (m, 3H, cyclohex-CH_2), 1.64-1.52 (m, 2H, cyclohex-CH_2), 1.44-1.32 (m, 1H, cyclohex-CH_2); ^{13}C NMR ($CDCl_3$, 100 MHz): δ (ppm) 160.8, 160.5, 149.1, 143.8, 141.7, 134.5, 133.6, 133.2, 132.9, 131.9, 130.8, 130.4, 128.6, 127.1, 124.3, 121.6, 118.7, 117.1, 110.5 (ArC), 55.7 (cyclohex-CH), 33.2 (cyclohex-CH_2), 25.5 (cyclohex-CH_2), 25.2 (cyclohex-CH_2); MS (ESI): m/z 397.0 (M^++1); Anal Calcd for $C_{25}H_{20}N_2O_3$: C, 75.74; H, 5.09; N, 7.07; found C, 75.78; H, 5.05; N, 7.09.

View Article Online
DOI: 10.1039/C8OB02973C

6-(1-Cyclohexyl-1H-benzo[d]imidazol-6-yl)-1H,3H-benzo[de]isochromene-1,3-dione ***(9b)****:* Light brown solid; 70% yield; mp 193-196 ^{o}C; ^{1}H NMR ($CDCl_3$, 400 MHz): δ (ppm) 8.69 (d, J = 7.80 Hz, 1H, ArH), 8.67 (dd, ^{2}J = 7.32 Hz, ^{3}J = 0.92 Hz, 1H, ArH), 8.42 (d, J = 7.76 Hz, 1H, ArH), 8.15 (s, 1H, ArH), 7.97 (d, J = 8.24 Hz, 1H, ArH), 7.85 (d, J = 7.76 Hz, 1H, ArH), 7.79-7.75 (m, 1H, ArH), 7.56 (s, 1H, ArH), 7.41 (dd, ^{2}J = 8.24 Hz, ^{3}J = 1.36 Hz, 1H, ArH), 4.30-4.22 (m, 1H, cyclohex-CH), 2.29 (d, J = 11.00 Hz, 2H, cyclohex-CH_2), 2.01-1.96 (m, 2H, cyclohex-CH_2), 1.90-1.80 (m, 3H, cyclohex-CH_2), 1.56-1.45 (m, 2H, cyclohex-CH_2), 1.42-1.30 (m, 1H, cyclohex-CH_2); ^{13}C NMR ($CDCl_3$, 100 MHz): δ (ppm) 160.8, 160.6, 149.1, 141.7, 134.4, 133.4, 132.9, 132.1, 131.9, 130.8, 130.6, 128.7, 128.5, 128.4, 127.3, 124.1, 120.4, 118.8, 117.4, 111.4 (ArC), 55.6 (cyclohex-CH), 33.3 (cyclohex-CH_2), 25.6 (cyclohex-CH_2), 25.2 (cyclohex-CH_2); MS (ESI): m/z 397.0 (M^{+}+1); Anal Calcd for $C_{25}H_{20}N_2O_3$: C, 75.74; H, 5.09; N, 7.07; found C, 75.72; H, 5.11; N, 7.05.

6-(1-Cyclohexyl-1H-benzo[d]imidazol-5-yl)-1H-benzo[de]isoquinoline-1,3(2H)-dione ***(10a)****:* Light yellow solid; 20% yield; mp 208-211 ^{o}C; ^{1}H NMR ($CDCl_3$, 400 MHz): δ (ppm) 8.86 (s, 1H, NH), 8.66 (d, J = 7.32 Hz, 1H, ArH), 8.63 (d, J = 7.32 Hz, 1H, ArH), 8.39 (d, J = 8.72 Hz, 1H, ArH), 8.15 (s, 1H, ArH), 7.96 (s, 1H, ArH), 7.79 (d, J = 7.32 Hz, 1H, ArH), 7.71 (t, J = 7.80 Hz, 1H, ArH), 7.62 (d, J = 8.24 Hz, 1H, ArH), 7.44 (d, J = 8.24 Hz, 1H, ArH), 4.34-4.26 (m, 1H, cyclohex-CH), 2.32 (d, J = 12.80 Hz, 2H, cyclohex-CH_2), 2.05 (d, J = 13.20 Hz, 2H, cyclohex-CH_2), 1.94-1.85 (m, 3H, cyclohex-CH_2), 1.62-1.52 (m, 2H, cyclohex-CH_2), 1.42-1.32 (m, 1H, cyclohex-CH_2); ^{13}C NMR ($CDCl_3$, 100 MHz): δ (ppm) 164.2, 164.0, 148.2, 143.8, 141.6, 133.7, 133.4, 132.7, 130.9, 130.7, 130.6, 130.0, 128.2, 126.6, 124.6, 122.5, 121.8, 121.1, 110.3 (ArC), 55.7 (cyclohex-CH), 33.3 (cyclohex-CH_2), 25.6 (cyclohex-CH_2), 25.3 (cyclohex-CH_2); MS (ESI): m/z 396.1 (M^{+}+1); Anal Calcd for $C_{25}H_{21}N_3O_2$: C, 75.93; H, 5.35; N, 10.63; found C, 75.91; H, 5.37; N, 10.68.

6-(1-Cyclohexyl-1H-benzo[d]imidazol-6-yl)-1H-benzo[de]isoquinoline-1,3(2H)-dione ***(10b)****:* Light yellow solid; 25% yield; mp 213-216 ^{o}C; ^{1}H NMR ($CDCl_3$, 400 MHz): δ (ppm) 8.78 (s, 1H, NH), 8.67-8.63 (m, 2H, ArH), 8.35 (d, J = 8.24 Hz, 1H, ArH), 8.14 (s, 1H, ArH), 7.97 (d, J = 8.24 Hz, 1H, ArH), 7.81 (d, J = 7.80 Hz, 1H, ArH), 7.74 (t, J = 7.80 Hz, 1H, ArH), 7.55 (s, 1H, ArH), 7.41 (d, J = 7.80 Hz, 1H, ArH), 4.29-4.21 (m, 1H, cyclohex-CH), 2.29 (d, J = 11.00 Hz, 2H, cyclohex-CH_2), 2.01-1.96 (m, 2H, cyclohex-CH_2), 1.89-1.79 (m, 3H, cyclohex-CH_2), 1.55-1.42 (m, 2H, cyclohex-CH_2), 1.37-1.30 (m, 1H, cyclohex-CH_2); ^{13}C NMR ($CDCl_3$, 100 MHz): δ (ppm)

View Article Online
DOI: 10.1039/C8OB02973C

164.1, 163.8, 148.3, 133.6, 133.2, 131.9, 131.0, 130.8, 130.5, 129.9, 128.5, 128.4, 128.2, 126.8, 124.3, 122.6, 121.3, 120.3, 111.4 (ArC), 55.6 (cyclohex-CH), 33.3 (cyclohex-CH_2), 25.6 (cyclohex-CH_2), 25.2 (cyclohex-CH_2); MS (ESI): m/z 396.1 (M^++1); Anal Calcd for $C_{25}H_{21}N_3O_2$: C, 75.93; H, 5.35; N, 10.63; found C, 75.89; H, 5.39; N, 10.61.

*Synthesis of 2-aryl/alkyl-6-(1-cyclohexyl-1H-benzo[d]imidazol-yl)-1H-benzo[de]isoquinoline-1,3(2H)-dione (**11-26**):* 6-(3/4-Amino-4/3-(cyclohexylamino)phenyl)-1*H*,3*H*-benzo[*de*]isochromene-1,3-dione (**7a-b**) (1 mmol) and corresponding amines (1.2 mmol) in 5 ml ethanol were taken in oven dried round bottom flask and refluxed the reaction mixture for 12-15 h. After the completion of the reaction, solvent was evaporated under pressure followed by water (50 ml) was added and extracted with chloroform. Chloroform layer was dried over sodium sulphate. Crude product was further column purified using ethyl acetate and hexane as eluents to get the desired solid products.

*2-Allyl-6-(1-cyclohexyl-1H-benzo[d]imidazol-5-yl)-1H-benzo[de]isoquinoline-1,3(2H)-dione (**11**):* Reddish brown solid; 76% yield; mp 261-263 ^oC; ^1H NMR ($CDCl_3$, 400 MHz): δ (ppm) 8.68 (d, *J* = 7.80 Hz, 1H, ArH), 8.65 (d, *J* = 7.32 Hz, 1H, ArH), 8.36 (d, *J* = 8.68 Hz, 1H, ArH), 8.12 (s, 1H, ArH), 7.95 (s, 1H, ArH), 7.77 (d, *J* = 7.76 Hz, 1H, ArH), 7.70-7.67 (m, 1H, ArH), 7.61 (d, *J* = 8.24 Hz, 1H, ArH), 7.44 (dd, ^2J = 8.24 Hz, ^3J = 1.40 Hz,1H, ArH), 6.08-5.98 (m, 1H, allyl-CH), 5.36 (dd, ^2J = 17.44 Hz, ^3J = 1.40 Hz,1H, allyl-CH_2), 5.24 (dd, ^2J = 10.08 Hz, ^3J = 0.92 Hz,1H, allyl-CH_2), 4.85 (d, *J* = 5.52 Hz, 2H, allyl-CH_2), 4.33-4.26 (m, 1H, cyclohex-CH), 2.32 (d, *J* = 11.00 Hz, 2H, cyclohex-CH_2), 2.05 (d, *J* = 13.32 Hz, 2H, cyclohex-CH_2), 1.93-1.83 (m, 3H, cyclohex-CH_2), 1.62-1.51 (m, 2H, cyclohex-CH_2), 1.43-1.32 (m, 1H, cyclohex-CH_2); ^{13}C NMR ($CDCl_3$, 100 MHz): δ (ppm) 164.1, 163.9, 147.5, 143.8, 141.5, 133.4, 132.7, 132.0, 131.2, 130.9, 130.3, 128.7, 128.4, 128.2, 126.7, 124.6, 122.6, 121.7, 121.2, 117.3, 110.3 (ArC), 55.7 (cyclohex-CH), 42.3 (allyl-CH_2), 33.3 (cyclohex-CH_2), 25.6 (cyclohex-CH_2), 25.3 (cyclohex-CH_2); MS (ESI): m/z 436.1 (M^++1); Anal Calcd for $C_{28}H_{25}N_3O_2$: C, 77.22; H, 5.79; N, 9.65; found C, 77.20; H, 5.80; N, 9.63.

*6-(1-Cyclohexyl-1H-benzo[d]imidazol-5-yl)-2-(prop-2-yn-1-yl)-1H-benzo[de]isoquinoline-1,3(2H)-dione (**12**):* Yellow solid; 82% yield; mp 258-261 ^oC; ^1H NMR ($CDCl_3$, 400 MHz): δ (ppm) 8.71 (d, *J* = 7.80 Hz, 1H, ArH), 8.68 (d, *J* = 7.36 Hz, 1H, ArH), 8.37 (d, *J* = 8.28 Hz, 1H, ArH), 8.13 (s, 1H, ArH), 7.94 (s, 1H, ArH), 7.79 (d, *J* = 7.32 Hz, 1H, ArH), 7.71 (t, *J* = 8.24 Hz, 1H, ArH), 7.62 (d, *J* = 8.28 Hz, 1H, ArH), 7.44 (dd, ^2J = 8.24 Hz, ^3J = 0.92 Hz,1H, ArH), 5.00 (d,

View Article Online
DOI: 10.1039/C8OB02973C

J = 2.72 Hz, 2H, propagyl-CH_2), 4.33-4.26 (m, 1H, cyclohex-CH), 2.32 (d, *J* = 11.00 Hz, 2H, cyclohex-CH_2), 2.21 (t, *J* = 2.32 Hz, 1H, propagyl-CH), 2.05-2.02 (m, 2H, cyclohex-CH_2), 1.94-1.83 (m, 3H, cyclohex-CH_2), 1.62-1.51 (m, 2H, cyclohex-CH_2), 1.43-1.35 (m, 1H, cyclohex-CH_2); ^{13}C NMR ($CDCl_3$, 100 MHz): δ (ppm) 163.6, 163.3, 147.9, 143.9, 141.6, 133.5, 132.6, 131.5, 131.2, 130.4, 128.7, 128.2, 126.7, 124.6, 122.4, 121.8, 121.0, 110.3 (ArC), 78.6 (propargyl-C), 70.4 (propargyl-CH), 55.7 (cyclohex-CH), 33.3 (cyclohex-CH_2), 29.4 (propargyl-CH_2), 25.6 (cyclohex-CH_2), 25.3 (cyclohex-CH_2); MS (ESI): m/z 434.1 (M^++1); Anal Calcd for $C_{28}H_{23}N_3O_2$: C, 77.58; H, 5.35; N, 9.69; found C, 77.61; H, 5.32; N, 9.68.

*2-Butyl-6-(1-cyclohexyl-1H-benzo[d]imidazol-5-yl)-1H-benzo[de]isoquinoline-1,3(2H)-dione (**13**):* White solid; 86% yield; mp 254-257 °C; ^{1}H NMR ($CDCl_3$, 400 MHz): δ (ppm) 8.66 (d, *J* = 7.80 Hz, 1H, ArH), 8.63 (dd, ^2J = 7.32 Hz, ^3J = 0.92 Hz, 1H, ArH), 8.34 (dd, ^2J = 8.24 Hz, ^3J = 0.92 Hz, 1H, ArH), 8.12 (s, 1H, ArH), 7.95 (s, 1H, ArH), 7.77 (d, *J* = 7.32 Hz, 1H, ArH), 7.69 (t, *J* = 7.32 Hz, 1H, ArH), 7.61 (d, *J* = 8.72 Hz, 1H, ArH), 7.44 (dd, ^2J = 8.68 Hz, ^3J = 1.36 Hz, 1H, ArH), 4.33-4.25 (m, 1H, cyclohex-CH), 4.24 (t, *J* = 7.32 Hz, 2H, butyl-CH_2), 2.32 (d, *J* = 11.44 Hz, 2H, cyclohex-CH_2), 2.06-2.00 (m, 2H, cyclohex-CH_2), 1.93-1.83 (m, 3H, cyclohex-CH_2), 1.77-1.71 (m, 2H, cyclohex-CH_2), 1.61-1.35 (m, 5H, cyclohex-CH_2 & butyl-CH_2), 1.01 (t, 3H, *J* = 7.32 Hz, butyl-CH_3); ^{13}C NMR ($CDCl_3$, 100 MHz): δ (ppm) 164.3, 164.1, 147.3, 143.9, 141.5, 133.4, 132.9, 132.8, 131.0, 130.7, 130.3, 128.6, 128.1, 126.6, 124.6, 122.8, 121.8, 121.4, 110.2 (ArC), 55.7 (cyclohex-CH), 40.2 (butyl-CH_2), 33.3 (cyclohex-CH_2), 30.1 (butyl-CH_2), 25.6 (cyclohex-CH_2), 25.3 (cyclohex-CH_2), 20.3 (butyl-CH_2), 13.8 (butyl-CH_3); MS (ESI): m/z 452.1 (M^++1); Anal Calcd for $C_{29}H_{29}N_3O_2$: C, 77.14; H, 6.47; N, 9.31; found C, 77.18; H, 6.51; N, 9.38.

6-*(1-Cyclohexyl-1H-benzo[d]imidazol-5-yl)-2-(2-(dimethylamino)ethyl)-1H-benzo[de]isoquinoline-1,3(2H)-dione (**14**):* Light yellow solid; 80% yield; mp 260-263 °C; ^{1}H NMR ($CDCl_3$, 400 MHz): δ (ppm) 8.59 (d, *J* = 7.76 Hz, 1H, ArH), 8.56 (d, *J* = 6.88 Hz, 1H, ArH), 8.33 (d, *J* = 8.28 Hz, 1H, ArH), 8.13 (s, 1H, ArH), 7.90 (s, 1H, ArH), 7.73 (d, *J* = 7.32 Hz, 1H, ArH), 7.65 (t, *J* = 8.24 Hz, 1H, ArH), 7.60 (d, *J* = 8.24 Hz, 1H, ArH), 7.39 (d, *J* = 8.24 Hz, 1H, ArH), 4.73 (t, *J* = 6.64 Hz, 2H, ethyl-CH_2), 4.33-4.25 (m, 1H, cyclohex-CH), 3.86 (t, *J* = 6.40 Hz, 2H, ethyl-CH_2), 3.51 (s, 6H, N-CH_3), 2.31 (d, *J* = 11.00 Hz, 2H, cyclohex-CH_2), 2.04 (d, *J* = 13.32 Hz, 2H, cyclohex-CH_2), 1.93-1.78 (m, 3H, cyclohex-CH_2), 1.61-1.51 (m, 2H, cyclohex-CH_2), 1.42-1.33 (m, 1H, cyclohex-CH_2); ^{13}C NMR ($CDCl_3$, 100 MHz): δ (ppm) 164.2, 164.0, 148.1, 143.8, 141.6, 133.6, 133.5, 132.4, 131.5, 131.2, 130.3, 128.6, 128.3, 126.8, 124.6, 122.0, 121.7,

View Article Online
DOI: 10.1039/C8OB02973C

120.5, 110.4 (ArC), 66.5 (ethyl-CH_2), 57.7 (N-CH_3), 55.7 (cyclohex-CH), 34.8 (ethyl-CH_2), 33.3 (cyclohex-CH_2), 25.6 (cyclohex-CH_2), 25.3 (cyclohex-CH_2); MS (ESI): m/z 467.1 (M^++1); Anal Calcd for $C_{29}H_{30}N_4O_2$: C, 74.65; H, 6.48; N, 12.01; found C, 74.62; H, 6.51; N, 12.05.

*6-(1-Cyclohexyl-1H-benzo[d]imidazol-5-yl)-2-(2-(diethylamino)ethyl)-1H-benzo[de]isoquinoline-1,3(2H)-dione (**15**):* Light yellow solid; 81% yield; mp 265-268 ^oC; ^1H NMR ($CDCl_3$, 400 MHz): δ (ppm) 8.66 (d, J = 7.36 Hz, 1H, ArH), 8.63 (d, J = 7.32 Hz, 1H, ArH), 8.35 (d, J = 8.24 Hz, 1H, ArH), 8.12 (s, 1H, ArH), 7.94 (s, 1H, ArH), 7.77 (d, J = 7.80 Hz, 1H, ArH), 7.69 (t, J = 7.80 Hz, 1H, ArH), 7.61 (d, J = 8.28 Hz, 1H, ArH), 7.44 (d, J = 8.24 Hz, 1H, ArH), 4.37 (t, J = 7.36 Hz, 2H, ethyl-CH_2), 4.32-4.25 (m, 1H, cyclohex-CH), 2.90 (t, J = 7.76 Hz, 2H, ethyl-CH_2), 2.78 (q, J = 7.32 Hz, 4H, ethyl-CH_2), 2.32 (d, J = 11.48 Hz, 2H, cyclohex-CH_2), 2.05 (d, J = 13.32 Hz, 2H, cyclohex-CH_2), 1.93-1.83 (m, 3H, cyclohex-CH_2), 1.62-1.50 (m, 2H, cyclohex-CH_2), 1.43-1.34 (m, 1H, cyclohex-CH_2), 1.17 (t, J = 6.88 Hz, 6H, ethyl-CH_3); ^{13}C NMR ($CDCl_3$, 100 MHz): δ (ppm) 164.3, 164.1, 147.5, 143.9, 141.5, 133.4, 133.1, 132.7, 131.1, 130.8, 130.3, 128.6, 128.2, 126.6, 124.6, 122.6, 121.7, 121.2, 110.2 (ArC), 55.7 (cyclohex-CH_2), 49.4 (ethyl-CH_2), 47.5 (ethyl-CH_2), 37.4 (ethyl-CH_2), 33.3 (cyclohex-CH_2), 25.6 (cyclohex-CH_2), 25.3 (cyclohex-CH_2), 11.86 (ethyl-CH_3); MS (ESI): m/z 495.1 (M^++1); Anal Calcd for $C_{31}H_{34}N_4O_2$: C, 75.28; H, 6.93; N, 11.33; found C, 75.25; H, 6.90; N, 11.36.

*6-(1-Cyclohexyl-1H-benzo[d]imidazol-5-yl)-2-(2-hydroxyethyl)-1H-benzo[de]isoquinoline-1,3(2H)-dione (**16**):* Light brown solid; 76% yield; mp 275-278 ^oC; ^1H NMR ($CDCl_3$, 400 MHz): δ (ppm) 8.67 (d, J = 7.32 Hz, 1H, ArH), 8.64 (dd, ^2J = 7.36 Hz, ^3J = 0.92 Hz, 1H, ArH), 8.36 (d, J = 8.72 Hz, 1H, ArH), 8.12 (s, 1H, ArH), 7.94 (s, 1H, ArH), 7.77 (d, J = 7.76 Hz, 1H, ArH), 7.70 (t, J = 8.24 Hz, 1H, ArH), 7.61 (d, J = 8.24 Hz, 1H, ArH), 7.44 (dd, ^2J = 8.72 Hz, ^3J = 1.40 Hz, 1H, ArH), 4.51 (t, J = 4.05 Hz, 2H, ethyl-CH_2), 4.32-4.26 (m, 1H, cyclohex-CH), 4.02 (t, J = 5.04 Hz, 2H, ethyl-CH_2), 2.31 (d, J = 11.00 Hz, 2H, cyclohex-CH_2), 2.05-2.02 (m, 2H, cyclohex-CH_2), 1.93-1.83 (m, 3H, cyclohex-CH_2), 1.61-1.52 (m, 2H, cyclohex-CH_2), 1.42-1.35 (m, 1H, cyclohex-CH_2); ^{13}C NMR ($CDCl_3$, 100 MHz): δ (ppm) 165.3, 165.1, 147.8, 143.7, 141.6, 133.4, 132.5, 131.4, 131.1, 130.2, 128.7, 128.2, 126.7, 124.6, 122.4, 121.7, 120.9, 110.3 (ArC), 61.7 (ethyl-CH_2), 55.2 (cyclohex-CH), 42.8 (ethyl-CH_2), 33.3 (cyclohex-CH_2), 25.6 (cyclohex-CH_2), 25.3 (cyclohex-CH_2); MS (ESI): m/z 440.0 (M^++1); Anal Calcd for $C_{27}H_{25}N_3O_3$: C, 73.79; H, 5.73; N, 9.56; found C, 73.84; H, 5.79; N, 9.59.

View Article Online
DOI: 10.1039/C8OB02973C

*2-(2-Aminoethyl)-6-(1-cyclohexyl-1H-benzo[d]imidazol-5-yl)-1H-benzo[de]isoquinoline-1,3(2H)-dione (**17**):* Brown solid; 71% yield; mp 270-273 ^{o}C; ^{1}H NMR ($CDCl_3$, 400 MHz): δ (ppm) 8.53-8.47 (m, 2H, ArH), 8.23 (t, *J* = 8.72 Hz, 1H, ArH), 8.11 (s, 1H, ArH), 7.93 (s, 1H, ArH), 7.68 (d, *J* = 6.40 Hz, 1H, ArH), 7.60-7.56 (m, 2H, ArH), 7.43 (d, *J* = 8.72 Hz, 1H, ArH), 4.31-4.19 (m, 5H, cyclohex-CH, ethyl-CH_2), 2.31 (d, *J* = 9.60 Hz, 2H, cyclohex-CH_2), 2.05 (d, *J* = 13.76 Hz, 2H, cyclohex-CH_2), 1.92-1.82 (m, 3H, cyclohex-CH_2), 1.61-1.51 (m, 2H, cyclohex-CH_2), 1.41-1.32 (m, 1H, cyclohex-CH_2); ^{13}C NMR ($CDCl_3$, 100 MHz): δ (ppm) 164.4, 164.1, 147.6, 143.8, 141.5, 133.3, 133.0, 131.1, 130.7, 130.4, 128.6, 128.2, 126.8, 124.3, 122.7, 121.4, 120.3, 111.3 (ArC), 56.1 (ethyl-CH_2), 55.5 (cyclohex-CH), 37.1 (ethyl-CH_2), 33.3 (cyclohex-CH_2), 25.6 (cyclohex-CH_2), 25.2 (cyclohex-CH_2); MS (ESI): m/z 439.0 (M^++1); Anal Calcd for $C_{27}H_{26}N_4O_2$: C, 73.95; H, 5.98; N, 12.78; found C, 73.91; H, 5.92; N, 12.74.

*6-(1-Cyclohexyl-1H-benzo[d]imidazol-5-yl)-2-(2-morpholinoethyl)-1H-benzo[de]isoquinoline-1,3(2H)-dione (**18**):* Brown solid; 81% yield; mp 259-262 ^{o}C; ^{1}H NMR ($CDCl_3$, 400 MHz): δ (ppm) 8.66 (d, *J* = 7.32 Hz, 1H, ArH), 8.63 (dd, ^{2}J = 7.36 Hz, ^{3}J = 0.92 Hz, 1H, ArH), 8.36 (dd, ^{2}J = 8.24 Hz, ^{3}J = 0.92 Hz, 1H, ArH), 8.12 (s, 1H, ArH), 7.95 (s, 1H, ArH), 7.78 (d, *J* = 7.32 Hz, 1H, ArH), 7.70 (t, *J* = 8.72 Hz, 1H, ArH), 7.62 (d, *J* = 8.28 Hz, 1H, ArH), 7.44 (dd, ^{2}J = 8.24 Hz, ^{3}J = 0.92 Hz, 1H, ArH), 4.40 (t, *J* = 6.88 Hz, 2H, ethyl-CH_2), 4.33-4.26 (m, 1H, cyclohex-CH), 3.71 (t, *J* = 4.60 Hz, 4H, morph-CH_2), 2.76 (t, *J* = 7.32 Hz, 2H, ethyl-CH_2), 2.63 (bs, 4H, morph-CH_2), 2.32 (d, *J* = 11.44 Hz, 2H, cyclohex-CH_2), 2.05-2.02 (m, 2H, cyclohex-CH_2), 1.94-1.85 (m, 3H, cyclohex-CH_2), 1.61-1.52 (m, 2H, cyclohex-CH_2), 1.42-1.35 (m, 1H, cyclohex-CH_2); ^{13}C NMR ($CDCl_3$, 100 MHz): δ (ppm) 164.4, 164.1, 147.5, 143.9, 141.6, 133.4, 133.1, 132.7, 131.1, 130.8, 130.3, 128.7, 128.2, 126.7, 124.6, 122.7, 121.8, 121.3, 110.3 (ArC), 66.9 (morph-CH_2), 56.1 (ethyl-CH_2), 55.7 (cyclohex-CH), 53.7 (morph-CH_2), 37.1 (ethyl-CH_2), 33.3 (cyclohex-CH_2), 25.6 (cyclohex-CH_2), 25.3 (cyclohex-CH_2); MS (ESI): m/z 509.1 (M^++1); Anal Calcd for $C_{31}H_{32}N_4O_3$: C, 73.21; H, 6.34; N, 11.02; found C, 73.18; H, 6.31; N, 11.05.

*2-Benzyl-6-(1-cyclohexyl-1H-benzo[d]imidazol-5-yl)-1H-benzo[de]isoquinoline-1,3(2H)-dione (**19**):* Off white solid; 83% yield; mp 261-263 ^{o}C; ^{1}H NMR ($CDCl_3$, 400 MHz): δ (ppm) 8.67 (d, *J* = 7.36 Hz, 1H, ArH), 8.64 (dd, ^{2}J = 7.32 Hz, ^{3}J = 0.92 Hz, 1H, ArH), 8.34 (d, *J* = 8.24 Hz, 1H, ArH), 8.12 (s, 1H, ArH), 7.93 (s, 1H, ArH), 7.76 (d, *J* = 7.32 Hz, 1H, ArH), 7.68 (t, *J* = 7.32 Hz, 2H, ArH), 7.60-7.55 (m, 3H, ArH), 7.43 (dd, ^{2}J = 8.24 Hz, ^{3}J = 0.92 Hz, 1H, ArH), 7.32 (t, *J* = 7.36 Hz, 2H, ArH), 5.41 (s, 2H, benzyl-CH_2), 4.32-4.24 (m, 1H, cyclohex-CH), 2.31 (d, *J*

View Article Online
DOI: 10.1039/C8OB02973C

= 12.84 Hz, 2H, cyclohex-CH_2), 2.04-2.01 (m, 2H, cyclohex-CH_2), 1.92-1.82 (m, 3H, cyclohex-CH_2), 1.61-1.50 (m, 2H, cyclohex-CH_2), 1.42-1.37 (m, 1H, cyclohex-CH_2); ^{13}C NMR ($CDCl_3$, 100 MHz): δ (ppm) 164.3, 164.1, 147.5, 143.8, 141.5, 137.2, 133.1, 132.7, 132.0, 131.9, 131.3, 131.0, 130.3, 128.7, 128.3, 128.1, 127.3, 126.6, 124.6, 122.6, 121.7, 121.2, 110.3 (ArC), 55.7 (cyclohex-CH), 43.5 (benzyl-CH_2), 33.3 (cyclohex-CH_2), 25.6 (cyclohex-CH_2), 25.2 (cyclohex-CH_2); MS (ESI): m/z 486.1 (M^++1); Anal Calcd for $C_{32}H_{27}N_3O_2$: C, 79.15; H, 5.60; N, 8.65; found C, 79.11; H, 5.65; N, 8.61.

*6-(1-Cyclohexyl-1H-benzo[d]imidazol-5-yl)-2-(4-fluorophenyl)-1H-benzo[de]isoquinoline-1,3(2H)-dione (**20**):* Brown solid; 78% yield; mp 262-264 °C; ^{1}H NMR ($CDCl_3$, 400 MHz): δ (ppm) 8.70 (d, J = 7.32 Hz, 1H, ArH), 8.68 (dd, ^2J = 7.32 Hz, ^3J = 0.88 Hz, 1H, ArH), 8.42 (dd, ^2J = 8.24 Hz, ^3J = 0.92 Hz, 1H, ArH), 8.13 (s, 1H, ArH), 7.97 (d, J = 0.88 Hz, 1H, ArH), 7.81 (d, J = 7.36 Hz, 1H, ArH), 7.73 (t, J = 8.72 Hz, 1H, ArH), 7.63 (d, J = 8.24 Hz, 1H, ArH), 7.46 (dd, ^2J = 8.68 Hz, ^3J = 1.84 Hz, 1H, ArH), 7.35-7.30 (m, 2H, ArH), 7.27-7.23 (m, 2H, ArH), 4.34-4.26 (m, 1H, cyclohex-CH), 2.33 (d, J = 11.88 Hz, 2H, cyclohex-CH_2), 2.06 (d, J = 13.76 Hz, 2H, cyclohex-CH_2), 1.94-1.84 (m, 3H, cyclohex-CH_2), 1.63-1.51 (m, 2H, cyclohex-CH_2), 1.43-1.35 (m, 1H, cyclohex-CH_2); ^{13}C NMR ($CDCl_3$, 100 MHz): δ (ppm) 164.5, 164.3, 148.0, 143.9, 141.6, 133.5, 133.4, 132.6, 131.6, 131.3, 131.1, 130.5, 130.4, 130.3, 129.0, 128.3, 126.8, 124.6, 122.7, 121.8, 121.2, 116.5, 116.2, 110.3 (ArC), 55.7 (cyclohex-CH), 33.3 (cyclohex-CH_2), 25.6 (cyclohex-CH_2), 25.3 (cyclohex-CH_2); MS (ESI): m/z 490.1 (M^++1); Anal Calcd for $C_{31}H_{24}FN_3O_2$: C, 76.06; H, 4.94; N, 8.58; found C, 76.11; H, 4.97; N, 8.61.

*2-(Benzo[d]thiazol-2-yl)-6-(1-cyclohexyl-1H-benzo[d]imidazol-5-yl)-1H-benzo[de]isoquinoline-1,3(2H)-dione (**21**):* Light yellow solid; 75% yield; mp 269-272 °C; ^{1}H NMR ($CDCl_3$, 400 MHz): δ (ppm) 8.74 (d, J = 7.32 Hz, 1H, ArH), 8.71 (dd, ^2J = 7.32 Hz, ^3J = 0.92 Hz, 1H, ArH), 8.45 (dd, ^2J = 8.72 Hz, ^3J = 1.40 Hz, 1H, ArH), 8.17 (d, J = 7.80 Hz, 1H, ArH), 8.14 (s, 1H, ArH), 7.97 (d, J = 7.32 Hz, 2H, ArH), 7.82 (d, J = 7.80 Hz, 1H, ArH), 7.75 (t, J = 7.32 Hz, 1H, ArH), 7.63 (d, J = 8.04 Hz, 1H, ArH), 7.58-750 (m, 2H, ArH), 7.48-7.45 (m, 1H, ArH), 4.34-4.26 (m, 1H, cyclohex-CH), 2.32 (d, J = 11.00 Hz, 2H, cyclohex-CH_2), 2.05 (d, J = 14.24 Hz, 2H, cyclohex-CH_2), 1.94-1.84 (m, 3H, cyclohex-CH_2), 1.62-1.52 (m, 2H, cyclohex-CH_2), 1.42-1.33 (m, 1H, cyclohex-CH_2); ^{13}C NMR ($CDCl_3$, 100 MHz): δ (ppm) 163.8, 163.6, 155.8, 150.4, 148.6, 143.9, 141.7, 136.7, 134.2, 133.5, 132.5, 132.0, 131.6, 130.6, 129.2, 128.4, 126.8, 126.3, 126.0, 124.6, 124.2, 122.1, 121.8, 120.6, 110.4 (ArC), 55.7 (cyclohex-CH), 33.3(cyclohex-CH_2),

View Article Online
DOI: 10.1039/C8OB02973C

25.6 (cyclohex-CH_2), 25.3 (cyclohex-CH_2); MS (ESI): m/z 529.1 (M^++1); Anal Calcd for $C_{32}H_{24}N_4O_2S$: C, 72.71; H, 4.58; N, 10.60; S, 6.06; found C, 72.66; H, 4.65; N, 10.71; S, 6.09.

*3-(1-Cyclohexyl-1H-benzo[d]imidazol-5-yl)-7H-benzo[de]benzo[4,5]imidazo[2,1-a]isoquinolin-7-one (**22**):* Yellow solid; 80% yield; mp 281-283 °C; ^{1}H NMR ($CDCl_3$, 400 MHz): δ (ppm) 8.87 (t, *J* = 8.24 Hz, 1H, ArH), 8.82 (t, *J* = 7.80 Hz, 1H, ArH), 8.58-8.55 (m, 1H, ArH), 8.43-8.24 (m, 1H, ArH), 8.13 (d, *J* = 2.28 Hz, 1H, ArH), 7.99 (d, *J* = 3.68 Hz, 1H, ArH), 7.90-7.87 (m, 1H, ArH), 7.81 (q, *J* = 4.12 Hz, 1H, ArH), 7.73-7.67 (m, 1H, ArH), 7.63 (dd, ^2J = 8.24 Hz, ^3J = 3.20 Hz, 1H, ArH), 7.50-7.45 (m, 3H, ArH), 4.34-4.26 (m, 1H, cyclohex-CH), 2.33 (d, *J* = 11.44 Hz, 2H, cyclohex-CH_2), 2.05 (d, *J* = 13.72 Hz, 2H, cyclohex-CH_2), 1.93-1.85 (m, 3H, cyclohex-CH_2), 1.63-1.51 (m, 2H, cyclohex-CH_2), 1.43-1.35 (m, 1H, cyclohex-CH_2); ^{13}C NMR ($CDCl_3$, 100 MHz): δ (ppm) 160.8, 160.7, 149.5, 148.6, 145.3, 143.9, 141.6, 134.3, 133.3, 132.9, 131.7, 131.6, 131.2, 131.0, 128.6, 128.3, 127.0, 126.7, 125.7, 125.1, 124.9, 121.9, 119.8, 115.8, 110.2 (ArC), 55.7 (cyclohex-CH), 33.3 (cyclohex-CH_2), 25.6 (cyclohex-CH_2), 25.3 (cyclohex-CH_2); MS (ESI): m/z 469.0 (M^++1); Anal Calcd for $C_{31}H_{24}N_4O$: C, 79.46; H, 5.16; N, 11.96; found C, 79.55; H, 5.13; N, 11.99.

*6-(1-Cyclohexyl-1H-benzo[d]imidazol-6-yl)-2-(2-(dimethylamino)ethyl)-1H-benzo[de]isoquinoline-1,3(2H)-dione (**23**):* Light yellow solid; 81% yield; mp 260-263 °C; ^{1}H NMR ($CDCl_3$, 400 MHz): δ (ppm) 8.66 (d, *J* = 7.32 Hz, 1H, ArH), 8.64 (d, *J* = 7.32 Hz, 1H, ArH), 8.30 (d, *J* = 7.80 Hz, 1H, ArH), 8.12 (s, 1H, ArH), 7.94 (d, *J* = 8.24 Hz, 1H, ArH), 7.78 (d, *J* = 7.80 Hz, 1H, ArH), 7.71 (t, *J* = 8.24 Hz, 1H, ArH), 7.54 (d, *J* = 0.68 Hz, 1H, ArH), 7.40 (dd, ^2J = 8.28 Hz, ^3J = 0.92 Hz, 1H, ArH), 4.44 (t, *J* = 6.68 Hz, 2H, ethyl-CH_2), 4.28-4.21 (m, 1H, cyclohex-CH), 2.88 (t, *J* = 7.12 Hz, 2H, ethyl-CH_2), 2.49 (s, 6H, N-CH_3), 2.28 (d, *J* = 11.00 Hz, 2H, cyclohex-CH_2), 2.00 (d, *J* = 13.72 Hz, 2H, cyclohex-CH_2), 1.89-1.79 (m, 3H, cyclohex-CH_2), 1.56-1.44 (m, 2H, cyclohex-CH_2), 1.40-1.31 (m, 1H, cyclohex-CH_2); ^{13}C NMR ($CDCl_3$, 100 MHz): δ (ppm) 164.4, 164.2, 147.6, 143.7, 141.5, 133.3, 133.0, 131.2, 130.8, 130.4, 128.7, 128.2, 126.8, 124.3, 122.6, 121.3, 120.2, 111.4 (ArC), 56.5 (ethyl-CH_2), 55.5 (cyclohex-CH), 45.1 (N-CH_3), 37.3 (ethyl-CH_2), 33.3 (cyclohex-CH_2), 25.5 (cyclohex-CH_2), 25.2 (cyclohex-CH_2); MS (ESI): m/z 467.1 (M^++1); Anal Calcd for $C_{29}H_{30}N_4O_2$: C, 74.65; H, 6.48; N, 12.01; found C, 74.71; H, 6.41; N, 12.12.

*6-(1-Cyclohexyl-1H-benzo[d]imidazol-6-yl)-2-(2-hydroxyethyl)-1H-benzo[de]isoquinoline-1,3(2H)-dione (**24**):* Brown solid; 76% yield; mp 275-278 °C; ^{1}H NMR ($CDCl_3$, 400 MHz): δ

View Article Online
DOI: 10.1039/C8OB02973C

(ppm) 8.57-8.48 (m, 2H, ArH), 8.20-8.15 (m, 2H, ArH), 7.94 (d, *J* = 8.68 Hz, 1H, ArH), 7.70 (d, *J* = 7.36 Hz, 1H, ArH), 7.64-7.59 (m, 1H, ArH), 7.54 (s, 1H, ArH), 7.41 (d, *J* = 9.16 Hz, 1H, ArH), 4.31-4.18 (m, 5H, cyclohex-CH & ethyl-CH_2), 2.29 (d, *J* = 11.00 Hz, 2H, cyclohex-CH_2), 1.99 (d, *J* = 13.28 Hz,, 2H, cyclohex-CH_2), 1.89-1.78 (m, 3H, cyclohex-CH_2), 1.55-1.47 (m, 2H, cyclohex-CH_2), 1.45-1.42 (m, 1H, cyclohex-CH_2); ^{13}C NMR ($CDCl_3$, 100 MHz): δ (ppm) 165.4, 165.2, 147.9, 141.4, 133.6, 132.7, 131.4, 131.1, 130.3, 128.5, 128.2, 126.8, 124.4, 122.3, 121.7, 120.7, 110.1 (ArC), 61.8 (ethyl-CH_2), 55.7 (cyclohex-CH), 42.8 (ethyl-CH_2), 33.3 (cyclohex-CH_2), 25.6 (cyclohex-CH_2), 25.2 (cyclohex-CH_2); MS (ESI): m/z 440.0 (M^++1); Anal Calcd for $C_{27}H_{25}N_3O_3$: C, 73.79; H, 5.73; N, 9.56; found C, 73.72; H, 5.78; N, 9.64.

*6-(1-Cyclohexyl-1H-benzo[d]imidazol-6-yl)-2-(2-morpholinoethyl)-1H-benzo[de]isoquinoline-1,3(2H)-dione (**25**):* Light brown solid; 83% yield; mp 259-262 °C; ^{1}H NMR ($CDCl_3$, 400 MHz): δ (ppm) 8.67 (d, *J* = 7.32 Hz, 1H, ArH), 8.65 (d, *J* = 7.32 Hz, 1H, ArH), 8.32 (d, *J* = 8.24 Hz, 1H, ArH), 8.13 (s, 1H, ArH), 7.96 (d, *J* = 8.24 Hz, 1H, ArH), 7.79 (d, *J* = 7.36 Hz, 1H, ArH), 7.73 (t, *J* = 7.32 Hz, 1H, ArH), 7.54 (s, 1H, ArH), 7.41 (d, *J* = 8.24 Hz, 1H, ArH), 4.41 (t, *J* = 6.64 Hz, 2H, ethyl-CH_2), 4.29-4.21 (m, 1H, cyclohex-CH), 3.72 (t, *J* = 4.60 Hz, 4H, morph-CH_2), 2.77 (t, *J* = 6.64 Hz, 2H, ethyl-CH_2), 2.64 (bs, 4H, morph-CH_2), 2.29 (d, *J* = 11.44 Hz, 2H, cyclohex-CH_2), 2.00 (d, *J* = 13.76 Hz, 2H, cyclohex-CH_2), 1.89-1.80 (m, 3H, cyclohex-CH_2), 1.56-1.44 (m, 2H, cyclohex-CH_2), 1.37-1.33 (m, 1H, cyclohex-CH_2); ^{13}C NMR ($CDCl_3$, 100 MHz): δ (ppm) 164.3, 164.1, 147.6, 143.8, 141.5, 133.6, 133.3, 133.0, 131.1, 130.7, 130.4, 128.6, 128.2, 126.8, 124.3, 122.7, 121.4, 120.3, 111.3 (ArC), 66.9 (morph-CH_2), 56.1 (ethyl-CH_2), 55.5 (cyclohex-CH), 53.7 (morph-CH_2), 37.1 (ethyl-CH_2), 33.3 (cyclohex-CH_2), 25.6 (cyclohex-CH_2), 25.2 (cyclohex-CH_2); MS (ESI): m/z 509.1 (M^++1); Anal Calcd for $C_{31}H_{32}N_4O_3$: C, 73.21; H, 6.34; N, 11.02; found C, 73.18; H, 6.42; N, 11.02.

*2-Benzyl-6-(1-cyclohexyl-1H-benzo[d]imidazol-6-yl)-1H-benzo[de]isoquinoline-1,3(2H)-dione (**26**):* Off whie solid; 77% yield; mp 266-269 °C; ^{1}H NMR ($CDCl_3$, 400 MHz): δ (ppm) 8.68 (d, *J* = 7.32 Hz, 1H, ArH), 8.66 (d, *J* = 7.76 Hz, 1H, ArH), 8.30 (d, *J* = 8.24 Hz, 1H, ArH), 8.12 (s, 1H, ArH), 7.95 (d, *J* = 8.72 Hz, 1H, ArH), 7.78 (d, *J* = 7.80 Hz, 1H, ArH), 7.72 (t, *J* = 8.72 Hz, 1H, ArH), 7.57 (t, *J* = 7.32 Hz, 3H, ArH), 7.40 (d, *J* = 8.24 Hz, 1H, ArH), 7.34 (t, *J* = 7.36 Hz, 3H, ArH), 5.42 (s, 2H, benzyl-CH_2), 4.28-4.20 (m, 1H, cyclohex-CH), 2.28 (d, *J* = 11.44 Hz, 2H, cyclohex-CH_2), 1.99 (d, *J* = 13.72 Hz, 2H, cyclohex-CH_2), 1.88-1.78 (m, 3H, cyclohex-CH_2), 1.55-1.44 (m, 2H, cyclohex-CH_2), 1.37-1.33 (m, 1H, cyclohex-CH_2); ^{13}C NMR ($CDCl_3$, 100 MHz): δ

View Article Online
DOI: 10.1039/C8OB02973C

(ppm) 164.3, 164.1, 147.6, 141.5, 137.2, 133.3, 133.0, 131.4, 130.9, 130.3, 128.8, 128.4, 128.2, 127.4, 126.7, 124.3, 122.7, 121.3, 120.2, 111.2 (ArC), 55.5 (cyclohex-CH), 43.5 (benzyl-CH_2), 33.3 (cyclohex-CH_2), 25.6 (cyclohex-CH_2), 25.2 (cyclohex-CH_2); MS (ESI): m/z 486.1 (M^++1); Anal Calcd for $C_{32}H_{27}N_3O_2$: C, 79.15; H, 5.60; N, 8.65; found C, 79.13; H, 5.61; N, 8.78.

Procedure for in vitro anticancer screening

The human tumor cell lines of the cancer screening panel are grown in RPMI 1640 medium containing 5% fetal bovine serum and 2 mM L-glutamine. Cells are inoculated into 96 well microtiter plates in 100 ml at plating densities ranging from 5,000 to 40,000 cells/well depending on the doubling time of individual cell lines. The microtiter plates are then incubated at 37 ˚C, 5% CO_2, 95% air and 100% relative humidity for 24 h.

After 24 h, two plates of each cell line are fixed in situ with TCA, to represent a measurement of the cell population for each cell line. Experimental drugs are solubilized in DMSO at 400-fold the desired final maximum test concentration and stored frozen prior to use. At the time of drug addition, an aliquot of frozen concentrate is thawed and diluted to twice the desired final maximum test concentration with complete medium containing 50 µg/ml gentamicin. Additional four, 10-fold or ½ log serial dilutions are made to provide a total of five drug concentrations plus control. Aliquots of 100 µL of these different drug dilutions are added to the appropriate microtiter wells, resulting in the required final drug concentrations. Following drug addition, the plates are incubated for an additional 48 h at 37 ˚C, 5% CO_2, 95% air, and 100% relative humidity. For adherent cells, the assay is terminated by the addition of cold TCA. Cells are fixed in situ by the gentle addition of 50 µL of cold 50% (w/v) TCA and incubated for 60 min at 4 ˚C. The supernatant is discarded, and the plates are washed five times with tap water and air dried. Sulforhodamine B (SRB) solution (100 µL) at 0.4% (w/v) in 1% acetic acid is added to each well, and plates are incubated for 10 min at room temperature. After staining, unbound dye is removed by washing five times with 1% acetic acid and the plates are air dried and then subsequently solubilized with 10 mM trizma base, and the absorbance is read on an automated plate reader at a wavelength of 515 nm. Using the seven absorbance measurements [time zero (T_z), control growth (C), and test growth in the presence of drug at the five concentration levels (T_i)], the percentage growth is calculated at each of the drug concentration levels. Percentage growth inhibition is calculated as:

[(Ti -Tz)/(C - Tz)] × 100 for concentrations for which $T_i \geq Tz$; [(Ti -Tz)/Tz] × 100 for concentrations for which Ti < Tz.

View Article Online
DOI: 10.1039/C8OB02973C

Three dose response parameters are calculated for each experimental agent. Growth inhibition of 50% (GI_{50}) is calculated from [(Ti -Tz)/(C - Tz)] × 100 = 50. The drug concentration resulting in total growth inhibition (TGI) is calculated from T_i = Tz. The LC_{50} is calculated from [(Ti-Tz)/Tz]×100 = 50.

DNA and BSA binding experiments

Sample preparation for DNA and BSA. Calf thymus (ct)-DNA (Sigma Chemicals) was dissolved in 10 mM Tris with 1 mM EDTA (*p*H 7.4). The purity of the DNA solution was checked by determining the absorbance ratio at 260 nm to 280 nm. Concentration of stock solution of DNA was measured by taking average extinction coefficient 6600 M^{-1} cm^{-1} of a single nucleotide at 260 nm. The stock solutions (10^{-3} M) of compounds (**15** and **23**) were prepared in DMSO. The stock solution of BSA (Sigma-Aldrich Chemical Co., USA) has been formed by dissolving solid BSA in 0.1 M phosphate buffer at *p*H 7.4 and was stored at 0-4 ˚C.

UV-Visible Spectroscopic. The DNA interactions were performed in the presence of fixed concentration of compounds **15** and **23** (20 μM) and titrated with varying concentration of ct-DNA (**15**; 0-110 μM, **23**; 0–85 μM). Phosphate buffer (*p*H 7.4) has been used to make the final volume to 1 ml.

The BSA interaction studies were performed in the presence of fixed concentration of BSA (7.0 μM) and titrated with different concentration of compounds **15** and **23** (0-15 μM). Phosphate buffer (*p*H 7.4) has been used to make the final volume to 3 ml.

For both DNA and BSA studies, base line corrections were carried out with blank solution containing phosphate buffer. All the UV-visible spectra have been recorded in the wavelength range 200–800 nm. Benesi-Hildebrand equation (1) was used to calculate the binding constants (K_b):

$$\frac{A_0}{A - A_0} = \frac{\varepsilon f}{\varepsilon b - \varepsilon f} + \frac{\varepsilon f}{\varepsilon b - \varepsilon f K_b[Analyte]} \quad \text{---------- (1)}$$

Where A_o is the initial absorbance of the free compound/BSA, A is the absorbance of the compound/BSA in the presence of analyte (ct-DNA or compound), ε_f and ε_b are molar extinction coefficients of the compound or BSA in its free and fully bound forms, respectively.

DNA melting experiments. DNA melting studies were performed by observing the absorption spectra of ct-DNA (8.5 μM) at the wavelength of 260 nm in the presence of compounds (**15** and **23**) (10 μM) at different temperatures using UV-visible spectrophotometer coupled with a thermostat. Phosphate buffer (*p*H 7.4) has been used to make the final volume to 1 ml. The

View Article Online
DOI: 10.1039/C8OB02973C

absorbance was determined as a function of temperature observing from 25 ˚C to 100 ˚C. The DNA melting temperature (T_m) was observed to be the transition midpoint.

Fluorescence spectroscopic. The DNA interaction experiment was carried out by titrating the fixed amount of compounds **15** and **23** (5.0 μM) at different temperatures (298 K, 308 K, and 318 K) with varying concentrations of ct-DNA (**15**; 298 K:0-60 μM, 308 K:0-35 μM, 318 K:0-35 μM, **23**; 298 K:0-35 μM, 308 K:0-25 μM, 318 K:0-30 μM). Phosphate buffer (pH 7.4) has been used to make the final volume to 1 ml.

The variation in fluorescence intensity was determined by titrating the fixed amount of BSA (7.0 μM) and varying the concentration of compounds **15** and **23** (0-45 μM) upon excitation at 280 nm. Phosphate buffer (pH 7.4) has been used to make the final volume to 3 ml.

All the spectra were observed in the wavelength range of 200–800 nm. The excitation and emission slit widths have been maintained constant throughout the experiment. Stern-Volmer equation-2 (equation-2) was used to find quenching process and to calculate the quenching constants

$$\frac{F_0}{F} = 1 + K_{sv}\,[\text{Analyte}] = 1 + K_q\tau_0[\text{Analyte}] \text{ ----------2}$$

Where F_o and F are the fluorescence intensities of compounds/BSA in the absence and presence of analyte (ct-DNA or compound), respectively.

Modified Stern-Volmer equation (Equation-3) was used to get the values of the binding constants (K_b) and the average number of binding sites (n).

$$\log\frac{F_0 - F}{F} = logK_b + nlog[analyte] \text{ ----------3}$$

The parameters are same as those of the Stern-Volmer equation.

To calculate the thermodynamic parameters i.e. the enthalpy change (ΔH) and entropy change (ΔS), the van't Hoff equation (Equation 4) was used.

$$logK_b = -\frac{\Delta H}{2.303RT} + \frac{\Delta S}{2.303R} \text{ ---------- 4}$$

Where K_b, T and R are the binding constant, absolute temperature and gas constant, respectively. In addition, the free energy change (ΔG) for the binding of analyte at different temperatures was calculated using the following equation (5).

$$\Delta G = \Delta H - T\Delta S \text{ ----------5}$$

Competitive displacement assays. Ethidium bromide displacement assay was performed with addition of ligand to EB-DNA complex solution. The concentration of ethidium bromide 3 μM and DNA 30 μM was titrated with varying concentration of ligands (**15**; 0-150 μM, **23**; 0–120

View Article Online
DOI: 10.1039/C8OB02973C

μM). The emission spectra were recorded between 200 nm and 800 nm on excitation of EB-DNA complex at 520 nm.

Circular Dichroism (CD) experiments. CD spectra of ct-DNA (40 μM) alone and complex (ct-DNA and ligands **15** and **23** at ratio of $r_{compound;ct\text{-}DNA)} = 0.025$) were determined using an CD spectrophotometer of Applied Photophysics. All the CD spectra have been observed in the range of 220 nm to 400 nm. The average of three scans was taken in all the experiments. The background spectrum of buffer solution (10 mM Tris-HCl, *p*H 7.4) was subtracted from the spectra of DNA and the ligand–DNA complex.

Cell cycle analysis. Cell cycle analysis was performed using flow cytometer. Cells (MDA-MB-468) were seeded in 6 well plates at a density of 10^5 cells/well in RPMI1640 medium. Cells were incubated for 24 h at 37 °C with 5% CO_2. Then medium was removed and added culture medium containing 1 μM concentration of compounds **15** and **23** along with control (without any compound) and incubated for 24 h. Propidium iodide (PI) was used for cell staining. For staining process, approx 10^6 cells were suspended in 0.5 mL of PBS and gently aspirated several times with a Pasteur pipet to obtain a mono-dispersed cell suspension, with minimal cell aggregation. Cells were fixed by transferring this suspension, with a Pasteur pipet, into centrifuge tubes containing 1 mL of 70% ethanol, on ice. Keep cells in ethanol for at least 2 h at 4°C. The ethanol-suspended cells were centrifuged for 5 min at 300g and then ethanol poured thoroughly. Suspended the cell pellet in 0.5 mL of PBS, for approx 30 s and centrifuged at 300g for 5 min. Suspended the cell pellet in 0.5 mL of PI staining solution. Kept in the dark at room temperature for 30 min. then transferred the sample to the flow cytometer and cell fluorescence was measured.

Associated content

Acknowledgments

KP thanks the DST-SERB, New Delhi (CRG/2018/002159). IS is grateful for CSIR, New Delhi (Project No. 09/677(0033)/2018-EMR-I) for SRF. NIH, Bethesda, USA for anticancer activities, SAI labs, TIET for NMR is also acknowledged. Authors thank to Punjab University, Chandigarh and IIT Ropar for providing mass facility. Authors also thanks to Aakaar Biotechnologies Private Limited, Lucknow for cell cycle analysis.

Supplementary data

Supplementary data related to this article can be found at

Author information

View Article Online
DOI: 10.1039/C8OB02973C

Corresponding author

E-mail kpaul@thapar.edu

Notes

The authors declare no competing financial interest.

References

1. L. H. Hurley, DNA and its associated processes as targets for cancer therapy. *Nat. Rev. Cancer* 2002, **2**, 188–200.

2. Z. F. Tao, L. Wang, K. D. Stewart, Z. H. Chen, W. Gu, M. H. Bui, P. Merta, H. Y. Zhang, P. Kovar, E. Johnson, C. Park, R. Judge, S. Rosenberg, T. Sowin, N. H. Lin, Structure-based design, synthesis, and biological evaluation of potent and selective macrocyclic checkpoint kinase 1 inhibitors. *J. Med. Chem.* 2007, **50**, 1514–1527.

3. H. H. Gong, D. Addla, J. S. Lv, C. H. Zhou, Heterocyclic naphthalimides as new skeleton structure of compounds with increasingly expanding relational medicinal applications. *Curr. Top. Med. Chem.* 2016, **16**, 3303-3364.

4. S. Banerjee, E. B. Veale, C. M. Phelan, S. A. Murphy, G. M. Tocci, L. J. Gillespie,; D. O. Frimannsson, J. M. Kelly, T. Gunnlaugsson, Recent advances in the development of 1,8-naphthalimide based DNA targeting binders, anticancer and fluorescent cellular imaging agents. *Chem. Soc. Rev.* 2013, **42**, 1601-1618.

5. J. S. Lv, X. M. Peng, B. Kishore, C. H. Zhou, 1,2,3-Triazole derived naphthalimides as a novel type of potential antimicrobial agents: Synthesis, antimicrobial activity, interaction with calf thymus DNA and human serum albumin. *Bioorg. Med. Chem. Lett.* 2014, **24**, 308-313.

6. F. J. Dai, Q. Li, Y. X. Wang, C. C. Ge, C. Y. Feng, S. Q. Xie, H. Y. He, X. J. Xu, C. J. Wang, Design, synthesis, and biological evaluation of mitochondria-targeted flavone-naphthalimide polyamine conjugates with antimetastatic activity. *J. Med. Chem.* 2017, **60,** 2071-2083.

7. M. F. Brana, A. Ramos, Naphthalimides as anti-cancer agents: Synthesis and biological activity. *Curr. Med. Chem. Anti-Cancer Agents* 2001, **1**, 237–255.

8. M. J. Ratain, R. Mick, F. Berezin, L. Janisch, R. L. Schilsky, N. J. Vogelzang, L. B. Lane, Phase I study of amonafide dosing based on acetylator phenotype. *Cancer Res.* 1993, **53**, 2304–2308.

9. M. F. Brana, M. Cacho, M. A. Garcia, B. de Pascual-Teresa, A. Ramos, M. T. Dominguez, J. M. Pozuelo, C. Abradelo, M. F. Rey-Stolle, M. Yuste, M. Banez-Coronel, J. C. Lacal, New

View Article Online
DOI: 10.1039/C8OB02973C

analogues of amonafide and elinafide, containing aromatic heterocycles: Synthesis, antitumor activity, molecular modeling, and DNA binding properties. *J. Med. Chem.* 2004, **47**, 1391–1399.

10. I. Antonini, G. Santoni, R. Lucciarini, C. Amantini, S. Sparapani, A. Magnano, Synthesis and biological evaluation of new asymmetrical bisintercalators as potential antitumor drugs. *J. Med. Chem.* 2006, **49**, 7198–7207.

11. E. Van Quaquebeke, T. Mahieu, P. Dumont, J. Dewelle, F. Ribaucour, G. Simon, S. Sauvage, J. F. Gaussin, J. Tuti, M. El Yazidi, F. Van Vynckt, T. Mijatovic, F. Lefranc, F. Darro, R. Kiss, 2,2,2-Trichloro-*N*-({2-[2-(dimethylamino)ethyl]-1,3-dioxo-2,3-dihydro-1*H*-benzo[*de*]isoquinolin5-yl}carbamoyl)acetamide (UNBS3157), a novel nonhematotoxic naphthalimide derivative with potent antitumor activity. *J. Med. Chem.* 2007, **50**, 4122–4134.

12. V. Tumiatti, A. Milelli, A. Minarini, M. Rosini, M. L. Bolognesi, M. Micco, V. Andrisano, M. Bartolini, F. Mancini, M. Recanatini, A. Cavalli, C. Melchiorre, Structure-activity relationships of acetylcholinesterase noncovalent inhibitors based on a polyamine backbone. Further investigation on the inner spacer. *J. Med. Chem.* 2008, **51**, 7308–7312.

13. Z. G. Li, Q. Yang, X. H. Qian, Novel thiazonaphthalimides as efficient antitumor and DNA photocleaving agents: Effects of intercalation, side chains, and substituent groups. *Bioorg. Med. Chem.* 2005, **13**, 4864–4870.

14. (a) Y. Bansal, O. Silakari, The therapeutic journey of benzimidazoles: A review, *Bioorg Med. Chem.* 2012, **20**, 6208-6236; (b) A. A. El Rashedy, H. Y. Aboul-Enein, Benzimidazole derivatives as potential anticancer agents. *Mini Rev. Med. Chem.* 2013, **13**, 399-407.

15. (a) V. A. Sontakke, A. N. Kate, S. Ghosh, P. More, R. Gonnade, N. M. Kumbhar, A. A. Kumbhar, B. A. Chopade, V. S. Shinde, Synthesis, DNA interaction and anticancer activity of 2-anthryl substituted benzimidazole derivatives. *New J. Chem.* 2015, **39,** 4882-4890; (b) A. Paul, S. Anbu, G. Sharma, M. L. Kuznetsov, B. Koch, M. F. C. G. da Silva, A. J. L. Pombeiro, Synthesis, DNA binding, cellular DNA lesion and cytotoxicity of a series of new benzimidazole-based Schiff base copper(II) complexes. *Dalton Trans*. 2015, **44**, 19983–19996; (c) Y. Miao, M. P. H. Lee, G. N. Parkinson, A. Batista-Parra, M. A. Ismail, S. Neidle, D. W. Boykin, W. D. Wilson, Out-of-Shape DNA minor groove binders: Induced fit interactions of heterocyclic dications with the DNA minor groove. *Biochemistry* 2005, **44,** 14701-14708; (d) A. Paul, Y. Chai, D. W. Boykin, W. D. Wilson, Understanding mixed sequence DNA recognition by novel

View Article Online
DOI: 10.1039/C8OB02973C

designed compounds: The kinetic and thermodynamic behavior of azabenzimidazole diamidines. *Biochemistry* 2015, **54**, 577−587; (e) L. Y. Sun, L. W. Zhu, Y. J. Tang, Increasing the distance between two monomers of topoisomerase IIβ under the action of antitumor agent 4β-sulfur-(benzimidazole) 4′-demethylepipodophyllotoxin. *Sci. Rep.* 2018, **8**, 14949-14958.

16. (a) K. Xu, P. M. Schwarz, R. F. Ludueña, Interaction of nocodazole with tubulin isotypes. *Drug Dev. Res.* 2002, **55**, 91–96; (b) A. M. Scutaru, M. Wenzel, H. Scheffler, G. Wolber, R. Gust, Optimization of the N-lost drugs melphalan and bendamustine: Synthesis and cytotoxicity of a new set of dendrimer-drug conjugates as tumor therapeutic agents. *Bioconjugate Chem.* 2010, **21**, 1728–1743; (c) L. A. Hammond, K. Davidson, R. Lawrence, J. B. Camden, D. D. Von Hoff, S. Weitman, E. Izbicka, Exploring the mechanisms of action of FB642 at the cellular level, *J. Cancer Res. Clin. Oncol.*, 2001, **127**, 301–313; (d) D. Hao, J. D. Rizzo, S. Stringer, R. V. Moore, J. Marty, D. L. Dexter, G. L. Mangold, J. B. Camden, D. D. Von Hoff, S. D. Weitman, Preclinical antitumor activity and pharmacokinetics of methyl-2-benzimidazolecarbamate (FB642), *Invest. New. Drugs*, 2000, **20**, 261–270; (e) C. K. Donawho, Y. Luo, Y. Luo, T. D. Penning, J. L. Bauch, J. J. Bouska, V. D. Bontcheva-Diaz, B. F. Cox, T. L. DeWeese, L. E. Dillehay, D. C. Ferguson, N. S. Ghoreishi-Haack, D. R. Grimm, R. Guan, E. K. Han, R. R. Holley-Shanks, B. Hristov, K. B. Idler, K. Jarvis, E. F. Johnson, L. R. Kleinberg, V. Klinghofer, L. M. Lasko, X. Liu, K. C. Marsh, T. P. McGonigal, J. A. Meulbroek, A. M. Olson, J. P. Palma, L. E. Rodriguez, Y. Shi, J. A. Stavropoulos, A. C. Tsurutani, G. D. Zhu, S. H. Rosenberg, V. L. Giranda, D. J. Frost, ABT-888, an orally active poly(ADP-Ribose) polymerase inhibitor that potentiates DNA-damaging agents in preclinical tumor models, *Clin. Cancer Res.,* 2007, **13**, 2728–2737.

17. P. Pantziarka, G. Bouche, L. Meheus, V. Sukhatme, V. P. Sukhatme, Repurposing drugs in oncology (ReDO)-mebendazole as an anti-cancer agent. *Ecancermedicalscience* 2014, **8**, 443-459.

18. (a) A. Kamal, N. R. Bolla, P. S. Srikanth, A. K. Srivastava, Naphthalimide derivatives with therapeutic characteristics: A patent review. *Expert Opin. Ther. Patents* 2013, **23**, 299-317; (b) H. H. Gong, D. Addla, J. S. Lv, C. H. Zhou, Heterocyclic naphthalimides as new skeleton structure of compounds with increasingly expanding relational medicinal applications. *Curr. Top. Med. Chem.* 2016, **16**, 3303-3364; (c) R. Tandon, V. Luxami, H. Kaur, N. Tandon, K. Paul, 1,8-Naphthalimide: A potent DNA intercalator and target for cancer therapy. *Chem. Rec.*

View Article Online
DOI: 10.1039/C8OB02973C

2017, **17**, 956–993; (d) M. D. Tomczyk, K. Z. Walczak, l,8-Naphthalimide based DNA intercalators and anticancer agents. A systematic review from 2007 to 2017. *Eur. J. Med. Chem.* 2018, **24**, 393-422.

19. (a) I. Ott, X. Qian, Y. Xu, D. H. W. Vlecken, I. J. Marques, D. Kubutat, J. Will, W. S. Sheldrick, P. Jesse, A. Prokop, C. P. Bagowski, A gold(I) phosphine complex containing a naphthalimide ligand functions as a TrxR inhibiting antiproliferative agent and angiogenesis inhibitor. *J. Med. Chem.* 2009, **52**, 763–770; (b) M. Verma, V. Luxami, K. Paul, Synthesis, *in vitro* evaluation and DNA interaction studies of *N*-allyl naphthalimide analogues as anticancer agents. *RSC Adv.* 2015, **5**, 41803-41813; (c) M. Verma, V. Luxami, K. Paul, Synthesis, *in vitro* evaluation and molecular modelling of naphthalimide analogue as anticancer agents, *Eur. J. Med. Chem.* 2013, **68**, 352-360.

20. R. M. Stone, E. Mazzola, D. Neuberg, S. L. Allen, A. Pigneux, R. K. Stuart, M. Wetzler, D. Rizzieri, H. P. Erba, L. Damon, J. H. Jang, M. S. Tallman, K. Warzocha, T. Masszi, M. A. Sekeres, M. Egyed, H. A. Horst, D. Selleslag, S. R. Solomon, P. Venugopal, A. S. Lundberg, B. Powell, Phase III open-label randomized study of cytarabine in combination with amonafide L-malate or daunorubicin as induction therapy for patients with secondary acute myeloid leukemia. *J. Clin. Oncol.* 2015, **33**, 1252–1257.

21. (a) M. R. Grever, S. A. Sehepartz, B. A. Chabners, The National Cancer Institute: Cancer drug discovery and development program. *Semin. Oncol.* 1992, **19**, 622-638; (b) A. Monks, D. Schudiero, P. Skehan, R. Shoemaker, K. Paull, D. Vistica, C. Hose, J. Langley, P. Cronise, A. Vaigro-Wolff, M. Gray-Goodrich, H. Campbell, J. Mayo, M. J. Boyd, Feasibility of a high-flux anticancer drug screen using a diverse panel of cultured human tumor cell lines. *J. Natl. Cancer Inst.* 1991, **83**, 757-766; (c) M. R. Boyd, K. D. Paull, Some practical considerations and applications of the national cancer institute *in vitro* anticancer drug discovery screen. *Drug Dev. Res.* 1995, **34**, 91-109.

22. H. A. Benesi, J. H. Hildebrand, A spectrophotometric investigation of the interaction of iodine with aromatic hydrocarbons. *J. Am. Chem. Soc.* 1949, **71**, 2703–2707.

23. A. Garofalo, L. Goossens, B. Baldeyrou, A. Lemoine, S. Ravez, P. Six, M. H. David-Cordonnier, J. P. Bonte, P. Depreux, A. Lansiaux, J. F. O. Goossens, Design, synthesis, and DNA-binding of *N*-alkyl(anilino)quinazoline derivatives. *J. Med. Chem.* 2010, **53**, 8089–8103.

View Article Online
DOI: 10.1039/C8OB02973C

24. M. R. Eftink, C. A. Ghiron, Fluorescence quenching studies with proteins. *Anal. Biochem.* 1981, **114**, 199-227.

25. J. R. Lakowicz, G. Webber, Quenching of fluorescence by oxygen. Probe for structural fluctuations in macromolecules. *Biochemistry* 1973, **12**, 4161-4170.

26. M. Jiang, M. X. Xie, D. Zheng, Y. Liu, X. Y. Li, X. Chen, Spectroscopic studies on the interaction of cinnamic acid and its hydroxyl derivatives with human serum albumin. *J. Mol. Struct.* 2004, **692**, 71-80.

27. I. Haq, Thermodynamics of drug–DNA interactions. *Arch. Biochem. Biophys.* 2002, **403**, 1-15.

28. J. B. Lepecq, C. A. Paoletti, Fluorescent complex between ethidium bromide and nucleic acids physical-chemical characterization. *J. Mol. Biol*. 1967, **27**, 87-106.

29. M. Eriksson, B. Nordén, Linear and circular dichroism of drug-nucleic acid complexes. *Methods Enzymol.* 2001, **340**, 68-98

30. (a) A. Rodger, B. Norden, In circular dichroism and linear dichroism, Oxford University Press, New York, 1997, Chapter 2; (b) N. Berova, K. Nakanishi, R. W. Woody, Circular dichroism principles and applications, 2nd ed., Wiley-VCH, New York, 2000.

31. M. Hranjec, M. Kralj, I. Piantanida, M. Sedić, L. Šuman, K. Pavelić, G. K. Zamola, Novel cyano- and amidino-substituted derivatives of styryl-2-benzimidazoles and benzimidazo[1,2-a]quinolines. Synthesis, photochemical synthesis, DNA binding, and antitumor evaluation, part 3. J. *Med. Chem.* 2007, **50**, 5696-5711.

32. N. C. Garbett, P. A. Ragazzon, J. B. Chaires, Circular dichroism to determine binding mode and affinity of ligand–DNA interactions. *Nat. Protoc.* 2007, **2**, 3166–3172.

33. A. Kamal, A. V. S. Rao, M. V. P. S. Vishnuvardhan, T. S. Reddy, K. Swapna, C. Bagul, N. V. S. Reddy, V. Srinivasulu, Synthesis of 2-anilinopyridyl–triazole conjugates as antimitotic agents. *Org. Biomol. Chem*. 2015, **13**, 4879-4895.

34. J. C. Pessoa, I. Tomaz, Transport of therapeutic vanadium and ruthenium complexes by blood plasma components. *Curr. Med. Chem.* 2010, **17**, 3701–3738.

35. The U.S. Food and Drug Administration website, retrieved on March 20, 2012, http://www.fda.gov/OHRMS/DOCKETS/ 98fr/00n-1269-nfr0001-03.pdf.

View Article Online
DOI: 10.1039/C8OB02973C

36. P. Mitra, U. Pal, N. C. Maiti, A. Ghosh, A. Anirban Bhunia, S. Basu, Identification of modes of interactions between 9-aminoacridine hydrochloride hydrate and serum proteins by low and high resolution spectroscopy and molecular modelling. *RSC Adv.* 2016**, 6,** 53454-53468.

37. V. Rajendiran, R. Karthik, M. Palaniandavar, V. S. Periasamy, M. A. Akbarsha, B. S. Srinag, H. Krishnamurthy, Mixed-ligand copper(II)-phenolate complexes: Effect of coligand on enhanced DNA and protein binding, DNA cleavage, and anticancer activity. *Inorg. Chem.* 2007, **46**, 8208–8221.

38. F. Maya, J. M. Tour, Synthesis of terphenyl oligomers as molecular electronic device candidates. *Tetrahedron*, 2004, **60**, 81-92.